Human Bone Marrow-Derived Myeloid Dendritic Cells Show an Immature Transcriptional and Functional Profile Compared to Their Peripheral Blood Counterparts and Separate from Slan+ Non-Classical Monocytes

Nathalie van Leeuwen-Kerkhoff[1], Kristina Lundberg[2], Theresia M. Westers[1], Shahram Kordasti[3†], Hetty J. Bontkes[4], Malin Lindstedt[2], Tanja D. de Gruijl[5] and Arjan A. van de Loosdrecht[1*]

[1] Cancer Center Amsterdam, Department of Hematology, VU University Medical Center, Amsterdam, Netherlands, [2] Department of Immunotechnology, Lund University, Lund, Sweden, [3] Department of Haematological Medicine, King's College London, London, United Kingdom, [4] Department of Pathology, VU University Medical Center, Amsterdam, Netherlands, [5] Cancer Center Amsterdam, Department of Medical Oncology, VU University Medical Center, Amsterdam, Netherlands

The human bone marrow (BM) gives rise to all distinct blood cell lineages, including CD1c+ (cDC2) and CD141+ (cDC1) myeloid dendritic cells (DC) and monocytes. These cell subsets are also present in peripheral blood (PB) and lymphoid tissues. However, the difference between the BM and PB compartment in terms of differentiation state and immunological role of DC is not yet known. The BM may represent both a site for development as well as a possible effector site and so far, little is known in this light with respect to different DC subsets. Using genome-wide transcriptional profiling we found clear differences between the BM and PB compartment and a location-dependent clustering for cDC2 and cDC1 was demonstrated. DC subsets from BM clustered together and separate from the corresponding subsets from PB, which similarly formed a cluster. In BM, a common proliferating and immature differentiating state was observed for the two DC subsets, whereas DC from the PB showed a more immune-activated mature profile. In contrast, BM-derived slan+ non-classical monocytes were closely related to their PB counterparts and not to DC subsets, implying a homogenous prolife irrespective of anatomical localization. Additional functional tests confirmed these transcriptional findings. DC-like functions were prominently exhibited by PB DC. They surpassed BM DC in maturation capacity, cytokine production, and induction of CD4+ and CD8+ T cell proliferation. This first study on myeloid DC in healthy human BM offers new information on steady state DC biology and could potentially serve as a starting point for further research on these immune cells in healthy conditions as well as in diseases.

Keywords: dendritic cells, non-classical monocytes, bone marrow, peripheral blood, microarray analysis, cytokines

INTRODUCTION

The human bone marrow (BM) compartment is the main site of hematopoiesis. It harbors early progenitor cells as well as more differentiated cells that will enter the circulation in a later stage for homing to secondary lymphoid organs or effector sites to mediate their immune functions. The developmental pathway of the dendritic cell (DC) lineage in the BM has been extensively studied in mice (1–12). Later, human homologs of DC were identified and recently the differentiation from human BM precursors into DC was described (13–23). Increasing knowledge on the sequential development of common and early progenitors to committed and more differentiated precursors may support the understanding of normal and aberrant hematopoiesis. This is for instance exemplified by selective cell lineage depletion in primary immunodeficiencies such as seen in patients with GATA2 mutations (24–26). These patients clearly show reduced numbers of natural killer cells, B cells, and monocytes and in addition a total absence of all DC subsets. In contrast, the level of granulocytes is normal, indicating a block in differentiation from progenitor to the more developed stages. Only recently, the immediate precursor of human DC has been identified which may now explain these DC-restricted depletions. Lee and colleagues developed a culture system in which they were able to define the human DC developmental pathway (18). From a common human granulocyte-monocyte-DC progenitor to a more committed human monocyte-DC progenitor, they finally could identify the direct human common DC progenitor (hCDP). The presence of hCDP is restricted to the BM compartment where it gives rise to a migratory conventional DC precursor (pre-CDC) that then produces the two major types of human myeloid DC, CD1c+, and CD141+ (now called cDC2 and cDC1, respectively) (19, 27). Transcriptional heterogeneity within the pre-CDC pool further revealed the existence of pre-commitment for cDC2 or cDC1 DC (20). Examination of different human tissues showed that these pre-CDC were not only present in the BM but could also be found in peripheral blood (PB) and tonsils. In contrast, the immediate monocyte precursor was only detected in BM. In addition to the information on sequential precursor production, data on activation state and functional capacities in different stages of cell development may give further insights into healthy and altered immune responses. It is assumed that immature/precursor forms of DC, including cDC2 and cDC1, leave the BM and circulate through the PB to the lymphoid tissues. Previously published data indeed support the fact that these circulating precursors are less mature and differentiated than their counterparts in peripheral tissues (15, 24, 28).

In human, the effect of environmental signals on DC function in different tissues, such as spleen, thymus, PB, lung, and skin was studied before by Heidkamp and colleagues (29).

However, information on developmental state and functional differences of cDC2 and cDC1 DC between the human BM and PB compartment is not available.

In this study, we focused on myeloid DC in the healthy human BM compartment in steady state conditions and compared them with their PB equivalents. Slan+ non-classical monocytes, previously recognized as a DC-like subset and, therefore, probably more closely linked to conventional DC than classical monocytes, were also included in this analysis. Detailed genome-wide transcriptional analysis as well as comparative functional validation showed clear compartment-related differences. Hierarchical clustering implied a close relationship of BM-derived cDC2 and cDC1 DC. Both subsets clustered away from their PB equivalents. Differentiation pathways, cell proliferation, and cell cycle control genes were most prominent in BM DC, whereas immune effector-related transcripts were over-expressed in PB subsets. In contrast, transcriptional profile and immunological function of slan+ non-classical monocytes were less dependent on the environment as a homogenous profile in both compartments was demonstrated. BM- and PB-derived slan+ non-classical monocytes clustered closer together than with the DC subsets from their respective compartments. Thus, under steady state circumstances both myeloid DC subsets potentially form a residential BM population that are in an earlier developmental phase than their PB equivalents, whereas slan+ non-classical monocytes are possibly PB-derived and patrol the BM in an effector role.

MATERIALS AND METHODS

Sample Processing and Cell Isolation

Human BM was obtained after written informed consent from patients undergoing cardiac surgery in the VU University Medical Center Amsterdam, The Netherlands. Peripheral blood (buffy coat) was purchased from the Sanquin blood supply service (Amsterdam, The Netherlands). The study was approved by the local ethical committee and in accordance with the declaration of Helsinki. Mononuclear cells (MNCs) from both PB as well as from BM were isolated by density centrifugation using Ficoll-Paque medium (GE Healthcare, Uppsala, Sweden). For functional tests, conventional DC subsets (cDC2 and cDC1) were sorted from fresh samples with a BD FACSAria™ flow cytometer (BD Biosciences, San Jose, CA, USA), using a monoclonal antibody (mAb) cocktail consisting of CD1c-PE-Cy7 (eBioscience, San Diego, CA, USA), CD11c-PerCP-Cy5.5, CD14/CD19-APC-H7 (all, BD Biosciences), CD141-APC (Miltenyi Biotec, Utrecht, The Netherlands), and HLA-DR-V450 (BD Biosciences). Both cell subsets were identified in the CD11c+ and HLA-DR+ cell fraction. cDC2 cells were also gated as CD14−/CD19− (Figure S1A in Supplementary Material). For better recovery of viable cells, slan+ non-classical monocytes were isolated based on M-DC8 expression using a magnetic isolation kit (Miltenyi Biotec). For application in microarray experiments, all cell subsets were flowcytometrically sorted from four individual PB and four BM donors (non-paired samples). After an enrichment step, comprising magnetic depletion of CD3+ and CD19+ cells using microbeads (Miltenyi Biotec), cells were incubated with a mAb cocktail consisting of M-DC8-FITC (Miltenyi Biotec), CD16-PE (Beckman Coulter, Brea, USA), CD11c, CD1c, CD141, CD14, CD19, and CD45-KO (BD Biosciences, Figure S1B in Supplementary Material). Sorted cells routinely showed >92% purity and were stored in Trizol

(Life Technologies, Carlsbad, CA, USA) until further use for RNA extraction.

Cell Frequencies

The enumeration of different cell subtypes in BM and PB was performed after lysis of erythrocytes (BD Pharm Lyse, BD Biosciences). Samples were incubated with a mix of mAb: M-DC8-FITC, CD303-FITC (Miltenyi Biotec), CD16-PE, CD11c-PerCP-Cy5.5, CD1c-Pe-Cy7, CD141-APC, CD14-APC-H7,

CD19-APC-H7, HLA-DR-V450, and CD45-KO and analyzed on a flow cytometer (FACSCanto-II, BD Biosciences). Data analysis was done using FlowJo software (Tree star, Ashland, OR, USA). After debris and doublet exclusion, myeloid cell subsets were identified in the CD45+ compartment and further gated on CD1c, CD141, M-DC8, CD303, or CD14 expression. HLA-DR and CD11c were used for further selection of cell populations (**Figure 1A**). To exclude contamination of B cells in the CD14+ monocyte gate, back gating in CD45 vs side scatter plots was
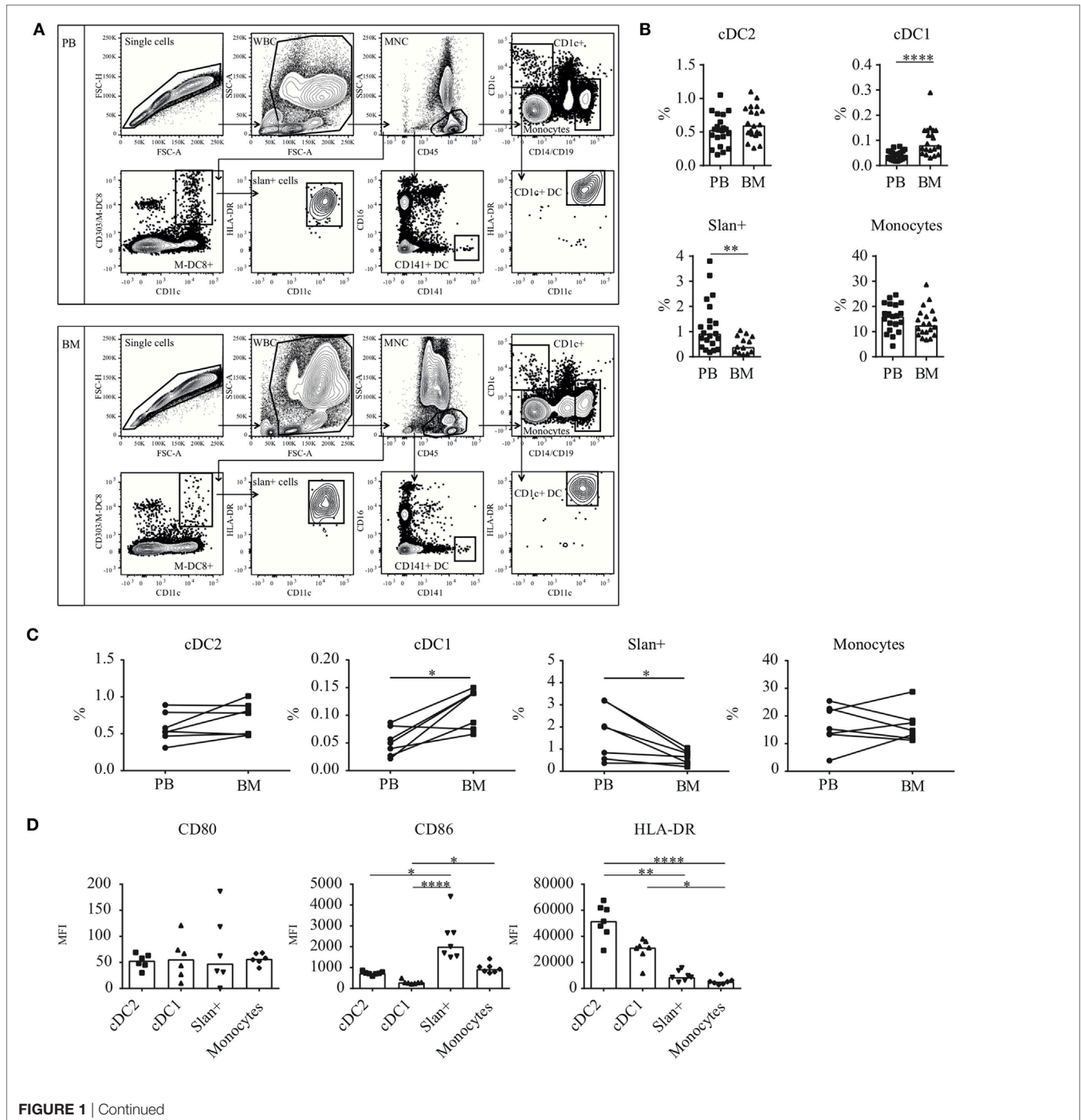

FIGURE 1 | Continued

FIGURE 1 | Dendritic cell (DC) and monocyte enumeration and baseline expression levels of (co-) stimulatory molecules in BM and PB. **(A)** Gating strategy for DC and monocyte subsets. CD45+ MNCs were gated after debris and doublet exclusion. Thereafter, cell subsets were identified based on the expression of CD1c (cDC2), CD141 (cDC1), or M-DC8 (slan+ non-classical monocytes). Classical monocytes were selected based on their high CD14 expression. **(B)** Frequencies of slan+ cells, monocytes, and the myeloid DC subsets cDC2 and cDC1 in human BM as compared to human PB. Percentages were calculated from the total CD45+ mononuclear cell fraction. Individual results and median percentages are shown for 17–21 (PB) and 13–20 (BM) healthy donors. Monocytes formed the main population in both compartments (PB, 16.0% and BM, 12.5%), followed by cDC2 (PB, 0.53% and BM, 0.60%) and slan+ non-classical monocytes (PB, 0.92% and BM, 0.39%). In BM as well as in PB, cDC1s were only present in low percentages (PB, 0.043% and BM, 0.081%). **(C)** Paired frequencies of PB and BM subsets, derived from one donor. A Wilcoxon matched-pairs signed rank test was performed to compare the PB and BM compartment ($n = 7$ donors, cDC2, and monocytes: no significant differences, cDC1 $p = 0.03$ and slan+ $p = 0.02$). **(D)** Baseline expression levels of HLA-DR ($n = 7$) and the co-stimulatory molecules CD80 ($n = 6$) and CD86 ($n = 7$) on BM-derived cell subsets. Individual experiments and median values are shown. **(E)** A comparison of baseline expression levels of three different activation markers between cell subsets from the PB ($n = 14–23$) and BM ($n = 6–7$) compartment. Histograms of the different markers of a representative donor and bar graphs of repeated experiments are shown. Median MFI values of individual stainings of the different cell subsets are compared between the two compartments. For CD80 and CD86, FMO controls are shown as a dotted line. Abbreviations: BM, bone marrow; PB, peripheral blood; WBC, white blood cells; MNC, mononuclear cells; MFI, median fluorescence intensity; FMO, fluorescence minus one. *$p < 0.05$, **$p < 0.01$, ***$p < 0.001$, and ****$p < 0.0001$.

used (data not shown in figure). Frequencies were calculated as percentages of CD45+ MNCs.

Preparation of cRNA and Gene Chip Hybridization

RNA was isolated from cDC2 (18,000–265,000 cells), cDC1 (1,000–17,300) and slan+ non-classical monocytes (9,000–150,000) and amplified using the Ovation Pico WTA System V2 (NuGen, San Carlos, CA, USA). Subsequently, RNA was labeled with the Encore Biotin Module Kit (NuGEN) according to manufacturer's protocols. Five microgram of the resulting labeled cDNA from each sample was hybridized to Human Transcriptome Arrays 2.0 microarrays (Affymetrix) and signals were scanned by Affymetrix GeneChip Scanner 3000 7G.

Microarray Data Analysis

Data analysis was performed as previously described (30). Briefly, microarray signals were normalized using the RMA algorithm

in the Affymetrix® Expression Console software (Affymetrix®) and quality checks and background noise correction were performed. Qlucore Omics Explorer 3.2 (Qlucore AB, Lund, Sweden) and Perseus were used for transcript filtering, identification of differentially expressed genes (DEGs; by performing an ANOVA analysis and using q-values of <0.05), heat map visualization, and Gene Set Enrichment Analysis (GSEA). Pathway analyses and interaction networks were created within the STRING v10.0 database (http://string-db.org/). The microarray data have been deposited in the GEO public database under Accession Number GSE112770.

Cell Staining, Maturation, and Cytokine Secretion

The intracellular expression of the proliferation marker Ki-67 was assessed in different cell subsets of the myeloid lineage by using a mAb panel consisting of the surface markers CD1c, CD11c, CD14, CD19, CD45, CD141, M-DC8, and HLA-DR, and,

a PE-conjugated mAb against the intracellular Ki-67 marker (BD Pharmingen). Unstimulated cell subsets of eight paired BM and PB samples were analyzed. After erythrocyte lysis, cell surface staining was performed. Thereafter, cells were fixed with phosphate-buffered saline containing 1% paraformaldehyde (PFA) and permeabilized by means of BD FACS Lysing solution (BD FACS Lysing Solution, BD Biosciences). Subsequently, the Ki-67 mAb was added and its intracellular expression in the different cell subsets was evaluated by flow cytometry (FACSCanto-II, BD Biosciences).

Baseline expression levels of co-stimulatory (CD80 and CD86) and minor histocompatibility (MHC)-class II (HLA-DR) molecules were evaluated before isolation of BM and PB cell subsets. Assessment of maturation capacity upon TLR-ligation by DC subsets and slan+ non-classical monocytes from both compartments was performed as described previously (30). Briefly, cells were isolated and pre-incubated for 4 h in Iscove's Modified Dulbecco's Medium supplemented with 10% fetal calf serum, 100 IU/ml penicillin, and 100 µg/ml streptomycin (all Gibco, Paisley, United Kingdom) at 37°C in a 5% CO_2 incubator. Thereafter, they were left unstimulated or were stimulated overnight with a combination of TLR ligands, i.e., LPS (100 ng/ml, Sigma-Aldrich, St. Louis, MO, USA) and R848 (3 µg/ml, Enzo Life Sciences, Farmingdale, USA) for cDC2 and slan+ non-classical monocytes, or Poly I:C (25 µg/ml, Sigma-Aldrich) and R848 for cDC1. The expression of respective markers was again measured by flow cytometry. Supernatants of these cultures were used for the detection of different cytokines by human enhanced sensitivity cytometric bead array (CBA) flex sets (BD Biosciences).

Allogeneic Mixed Leukocyte Reaction (MLR)

The capacity of DC subsets and slan+ non-classical monocytes to induce T cell proliferation was tested in an allogeneic MLR as described previously (30, 31). In brief, carboxyfluorescein succinimidyl ester (CFSE, Life Technologies, 1 µM)-labeled PB lymphocytes (PBL, i.e., CD14 depleted cell fraction) were co-cultured for 5 days with isolated and stimulated BM- or PB-derived slan+ monocytes or cDC2 in a ratio of 1:10. CFSE-dilution in CD4+ and CD8+ T cells was measured by flow cytometry.

Statistical Analysis

Graphpad Prism 6 software (San Diego, CA, USA) was used for non-microarray statistical data analysis. For two-group comparisons a non-parametric Mann–Whitney U test was performed, whereas for matched sample analyses a Wilcoxon signed rank test was used. For statistical differences a p-value of <0.05 was considered significant.

RESULTS

Quantitative Differences in Subsets Between the BM and PB

Dendritic cell and monocyte subsets were enumerated in the mononuclear cell fraction of fresh PB ($n = 17$–21) and BM ($n = 13$–20) samples from non-paired healthy donors (HD).

Cell populations were characterized by the expression of the cell-identifying markers CD1c and CD141 for the myeloid DC subsets. cDC2 were further defined as CD19−/CD14− and HLA-DR+/CD11c+. Slan+ cells, recently identified as the non-classical monocytes (30, 32), were characterized based on their CD11c and M-DC8 expression. Backgating in CD16 confirmed the expression of this marker on their cell surface (not shown). In contrast, classical monocytes did not express CD16, and were identified based on the high expression of CD14 (**Figure 1A**). B cell contamination was ruled out by creating back gating plots using discriminative CD45 expression and side scatter position of monocytes (not shown). In both compartments, all cell subsets could be found. Among these cells, CD14+classical monocytes accounted for the main population in PB as well as in BM (**Figure 1B**; PB, 16.0%; BM, 12.5%). Slan+ non-classical monocytes showed elevated numbers in PB compared to BM (PB, 0.92%. BM, 0.39%, $p = 0.0095$). In contrast, for cDC1, the frequency was significantly increased in the BM compared to PB (PB, 0.043%. BM, 0.081%, $p < 0.0001$). Comparable frequencies were detected for BM- and PB-derived cDC2 (PB, 0.53%; BM, 0.60%). In a set of 7 paired frequency analyses (PB and BM derived from the same donors), similar results were found for the different cell populations as compared to the larger unpaired cohort. For cDC1, increased percentages were seen in BM, whereas for slan+ non-classical monocytes all one-to-one comparisons showed elevated numbers in the PB compared to the BM (**Figure 1C**).

Extensive immunophenotypic information for DC and monocyte subsets in PB is available from previously published research (27, 30, 33–38). However, for human BM DC and monocytes these data are very limited (29). Therefore, the expression levels of important co-stimulatory and antigen-presenting molecules were assessed in BM-derived cells and compared to the expression levels on their PB counterparts. Similar to our observations for PB cell subsets (30), CD86 and HLA-DR were clearly expressed (at baseline, i.e., unstimulated expression) on DC and monocyte subsets. The expression of CD86 was higher on BM-derived monocyte subsets compared to BM-derived DC, whereas HLA-DR showed elevated levels on DC subsets (**Figure 1D**). Baseline expression levels of these markers were minimally different between BM and PB (**Figure 1E**). Only the HLA-DR expression on BM cDC2 was significantly higher compared to PB cDC2. For monocytes, CD86 levels were significantly higher in PB.

Transcriptomic-Based Clustering of DC Subsets but Not of Slan+ Non-Classical Monocytes Largely Depends on the Compartment They Reside in

For a better insight into the function of myeloid DC subsets (cDC2 and cDC1) in the BM compartment and to potentially identify compartment-related transcriptomic differences, an extensive genome-wide profiling study was performed. Both DC subsets as well as slan+ non-classical monocytes were sorted from fresh PB and BM of four individual HD. A total of 58,036 transcripts were found to be expressed. Principal component

analysis (PCA), using all expressed transcripts, showed a strong similarity of cell subsets between donors (**Figure 2A**). After applying an ANOVA test, 24,191 genes were found to be differentially expressed between all subsets in both compartments. Minimal spanning tree analysis revealed a compartment-based separation of cDC2 and cDC1. In contrast, slan+ non-classical monocytes from both compartments clustered closer together and separated from the DC subsets, irrespective of compartment (**Figure 2B**). Hierarchical clustering confirmed the separation for the conventional cDC2 and cDC1 subsets. Slan+ non-classical monocytes from PB and from BM grouped together (**Figure 2C**). Furthermore, slan+ non-classical monocytes were more closely related to PB DC than to BM DC subsets. The same analysis was repeated for DC only, without using slan+ monocytes. PCA and hierarchical clustering of all genes and 10114 DEGs showed similar results (Figure S2 in Supplementary Material). These findings suggest that transcriptional expression in myeloid DC subsets is more influenced by their environment (BM or PB) than by their intrinsic subset characteristics. In contrast, gene expression in slan+ non-classical monocytes appeared to be less dependent on environmental factors.

DC Subsets Display a Less Immune-Active Transcriptional Signature Than Slan+ Non-Classical Monocytes in the BM

Recent gene expression profile studies mainly focused on PB-derived cell types. For human BM-derived monocytes and DC, limited, if any, transcriptional information is available. Therefore, detailed gene expression profiles were analyzed in BM-derived slan+ non-classical monocytes, cDC2, and cDC1. From all expressed BM genes (58,459), differentially expressed transcripts between the three subsets were listed. Only if a gene was differentially over- or under-expressed in both comparative analyses (e.g., slan+ vs cDC2 and slan+ vs cDC1), it was considered to be subset-specific. Similar to our previous findings for PB subsets (30), BM-derived slan+ non-classical monocytes showed the highest number of unique transcripts. In total, 2,142 genes were differentially expressed in slan+ non-classical monocytes as compared to both DC subsets. From these DEGs, 965 were over-expressed and 1,177 were under-expressed. cDC2 showed 31 over-expressed and 14 under-expressed transcripts compared to the other two subsets. For cDC1 69 genes were found to be over-expressed and 54 to be under-expressed. Clustering of these DEGs in a heat map identified four gene clusters (**Figure 3A**, lower panel). Absolute expression levels of the identified DEGs offered further details of the possible biologically relevant differences between the subsets (**Figure 3B**). Consistent with our PB data (30), the top 100 over-expressed genes for slan+ non-classical monocytes contained recognized monocytic and immune-related genes, such as *FCGR3A/B*, *TLR4*, *C5AR1/2*, *C3AR1*, *CR1*, and *CX3CR1*. For cDC2, 25 genes with highest FC values are shown and for cDC1 60 genes. Also for the two BM-derived DC subsets well-known transcripts were found (*CD1c*, *CD163*, *MRC1*, and *CSF3R* for CD1c DC and *XCR1*, *CLEC9A*, and *IRF8* for CD141 DC), indicating a consistent expression of subset-defining genes in BM and PB.

Due to the limited number of over-expressed transcripts in cDC2 and cDC1, further pathway and interaction analyses were only performed for slan+ non-classical monocytes in order to
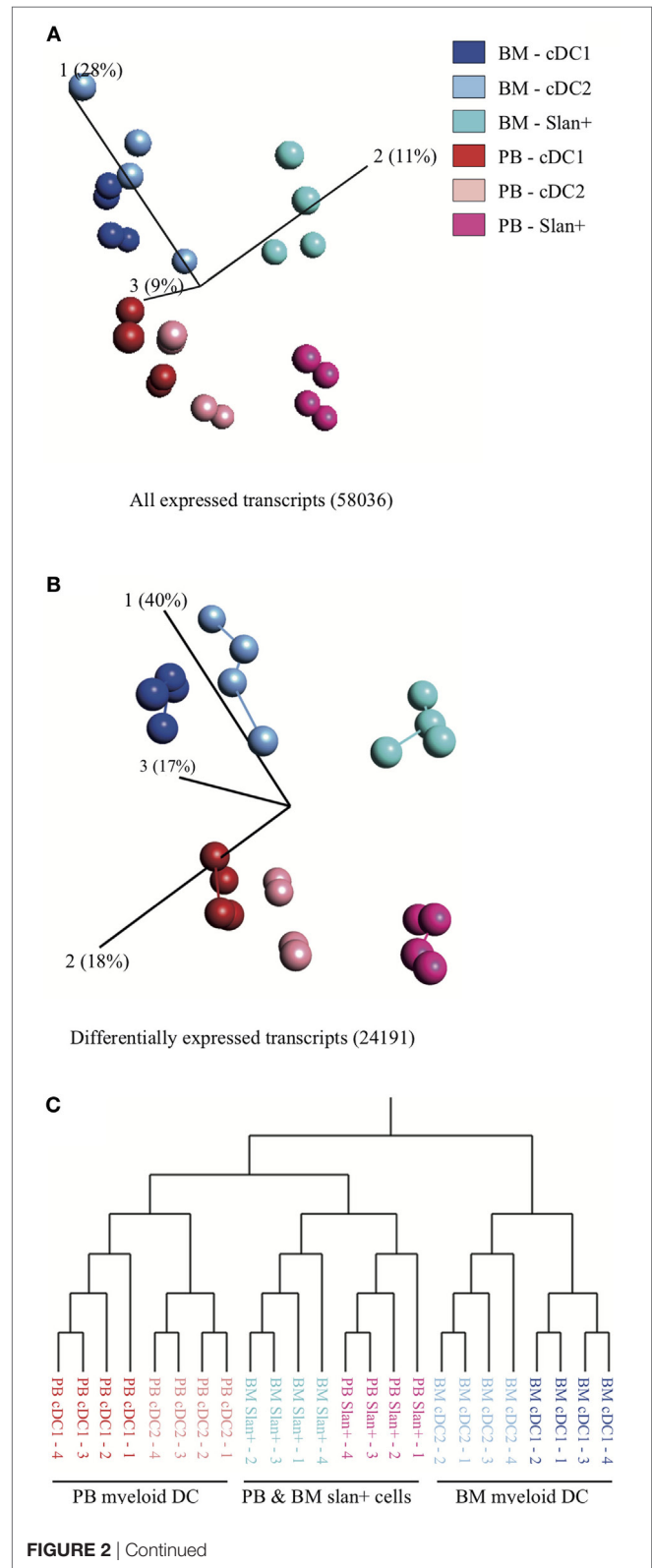

FIGURE 2 | Continued

find relevant biological context for these DEGs. Again, the top 100 highest FC values were used in this approach. They were imported in the STRING v10.0 database and a gene ontology (GO) term enrichment analysis was executed. The most enriched pathways mainly covered immune-related biological processes. As found for PB-derived slan+ non-classical monocytes (30), their BM counterparts also appeared to be highly involved in complement-mediated immune responses (**Figures 3C,D**). Enrichment analysis for under-expressed DEGs pointed to a lower involvement in adhesion and antigen processing and presentation (**Figure 3D**). Yet again, this shows great overlap with previous PB findings (30). Network interaction analysis of over-expressed DEGs showed a strong interaction of complement-related proteins as well as TLR-mediated signaling pathways (**Figure 3E**). For under-expressed DEGs a strong network of MHC-class II molecules was found (**Figure 3F**).

Gene Expression Profiles Are Dependent on Their Environment

To further delineate the distinct gene expression profiles for cDC2 and cDC1 in relation to their compartment (and in a lesser extent for slan+ monocytes), DEGs between PB and BM were identified for all three individual subsets. The highest number of differentially expressed transcripts between BM and PB was found for cDC2: in total 4,019 DEGs, of which 2,439 DEGs were over-expressed in BM and 1,580 over-expressed in PB. For cDC1 743 genes were over-expressed in BM and 436 in PB. Slan+ non-classical monocytes showed 998 genes to be over-expressed in BM and 847 in PB. Clustering of relative expression levels in each subset is depicted in **Figure 4A**. In order to translate these identified DEGs into a relevant biological meaning, lists of over- and under-expressed genes were loaded onto the STRING v10.0 pathway tool. For all three subsets, but most distinctly for cDC2 and cDC1, cell cycle and division processes were highly enriched in BM-derived subsets. Also metabolic cellular responses were significantly overrepresented in BM-derived cells (**Figure 4B**). Genes that were over-expressed in PB subsets were mainly involved in immune-related pathways, indicating a more differentiated and immunologically functional profile for cells circulating in this compartment (**Figure 4C**). To further confirm these findings a GSEA was performed for BM as well as for PB subsets. Using Kyoto Encyclopedia of Genes and Genomes pathways from the Broad Institute database an enrichment of pathways involved in cell cycle and replication was found for BM subsets. In contrast, immune-related pathways were enriched

in PB-derived subsets (**Figure 4D**). Again, confirming a distinct transcriptional profile of cell subsets in BM and PB.

Generation of a Gene Signature for DC Subsets That Is Environmentally Dependent

To establish a DC signature for BM as well as for PB, over-expressed gene lists (from the comparison BM vs PB) from both myeloid DC subsets were used. Since slan+ non-classical monocytes clearly form a non-DC-like population, they were excluded from this analysis. Using gene descriptions and GO biological process terms (e.g., cell cycle and immune response), transcripts involved in cellular and immunological processes were first selected for cDC2 as well as for cDC1. Relative expression levels of these transcripts are shown for BM and PB for both DC subsets (**Figure 5A**). From this selection, it is clear that transcripts that are involved in DNA replication, differentiation (i.e., *FLT3*), and cell cycle processes were evidently over-expressed in BM DC compared to PB DC. In contrast, cytokine signaling, adhesion, and endocytosis are terms that were overrepresented in PB DC. For PB cDC2, also co-stimulatory molecules such as CD40, CD80, and CD83 were expressed in higher levels compared to their BM equivalents. To further search for biologically relevant, and compartment-specific, DC gene signatures, Venn diagrams were created using gene lists of BM DC and PB DC. This revealed an overlap in over-expressed genes of 581 (22.3%) between BM cDC2 and BM cDC1 and 131 (6.9%) between PB cDC2 and PB cDC1 (**Figures 5B,C**), indicating a greater similarity between BM DC than between PB DC. Next, both overlapping genes lists were used for further pathway and network analysis in STRING v10.0. Pathways involved in cell cycle processes and cell division represented the overlapping transcripts in BM DC and formed the main biological function of these DC in this compartment (**Figure 5D**). In contrast, the overlapping transcripts in PB-derived DC could be found in pathways involving cell activation, differentiation, and antigen-receptor mediated signaling (**Figure 5E**). A network of these common PB-derived DC transcripts was generated (**Figure 5F**). Since the number of overlapping transcripts in BM DC was too high, a network could not be created.

Functional Analyses Confirm Transcriptional Findings

From the transcriptional profiling as described above it became clear that gene expression in myeloid DC subsets, and to a lesser extent in slan+ non-classical monocytes, was influenced by the compartment in which they reside. For functional validation of these findings, the expression of the Ki-67 protein, an intracellular marker for cell proliferation, was evaluated in a paired analysis of eight matched PB and BM samples. Consistent with our transcriptional analyses, for all subsets the percentage of Ki-67-positive cells was higher in BM than in PB and overall much higher in the DC subsets than in the slan+ non-classical monocytes. This was consistent for all donors (**Figure 6A**). Furthermore, DC-like functions, such as maturation capacity upon TLR-ligation, were tested for PB- and BM-derived cell subsets. Median fluorescence

intensity (MFI) of the co-stimulatory molecules CD80 and CD86, and, of HLA-DR at baseline and after overnight culture in the presence or absence of LPS and R848 (a combination of TLR ligands that has synergistic effects on cytokine production) (30, 39), were compared and fold change values were calculated (**Figure 6B**). Due to low cell yield, cDC1 could not be tested. The up-regulation of CD80 and CD86 was lower in BM-derived cDC2 as compared to their PB equivalents. In contrast, slan+ non-classical monocytes from BM and PB displayed a similar ability to enhance the expression levels of these molecules.

Next, the cytokine profile of slan+ non-classical monocytes and myeloid DC from the PB and BM compartment was assessed. Cells were stimulated overnight and by using CBA kits different cytokines were analyzed in culture supernatants. For stimulated cDC2 a remarkable difference was found between the PB and BM compartment (**Figure 6C**). Pro-inflammatory cytokines, in particular the Th-1-polarizing cytokine IL-12p70, were secreted in very low amounts by BM DC as compared to the corresponding subset in PB. A same trend was seen for cDC1 in stimulated conditions. Slan+ non-classical monocytes secreted negligible levels of IL-12p70 in PB and BM. In both compartments, they mainly produced IL-1β, IL-6, IL-8, and TNF, without significant differences between these two sites. Cell survival percentages

in these cultures could not be an underlying explanation for differences in cytokine secretion, since cultures showed equal live cell percentages for PB and BM-derived subsets (Figure S3 in Supplementary Material). To test the T cell priming and proliferation induction capacity, stimulated cDC2 and slan+ non-classical monocytes from both compartments were used in an allogeneic MLR. Again, cDC1 could not be used because of low cell numbers. In agreement with the transcriptional results, PB-derived cDC2 showed a superior induction capacity of T cell proliferation in CD4+ T cells as well as in CD8+ T cells compared to the BM-derived cDC2 (**Figure 6D**; Figure S4 in Supplementary Material). In contrast, but also confirming transcriptional data, slan+ non-classical monocytes did not show a significant difference between the compartments.

DISCUSSION

Dendritic cell subsets arise in the BM and leave this compartment in a more differentiated, but immature form, in order to supply the peripheral DC pool. The entire human DC development pathway has recently been elucidated and DC progenitors can now be immunophenotypically identified (40). The direct progeny of the circulating DC progenitors (pre-CDC) consists of the well
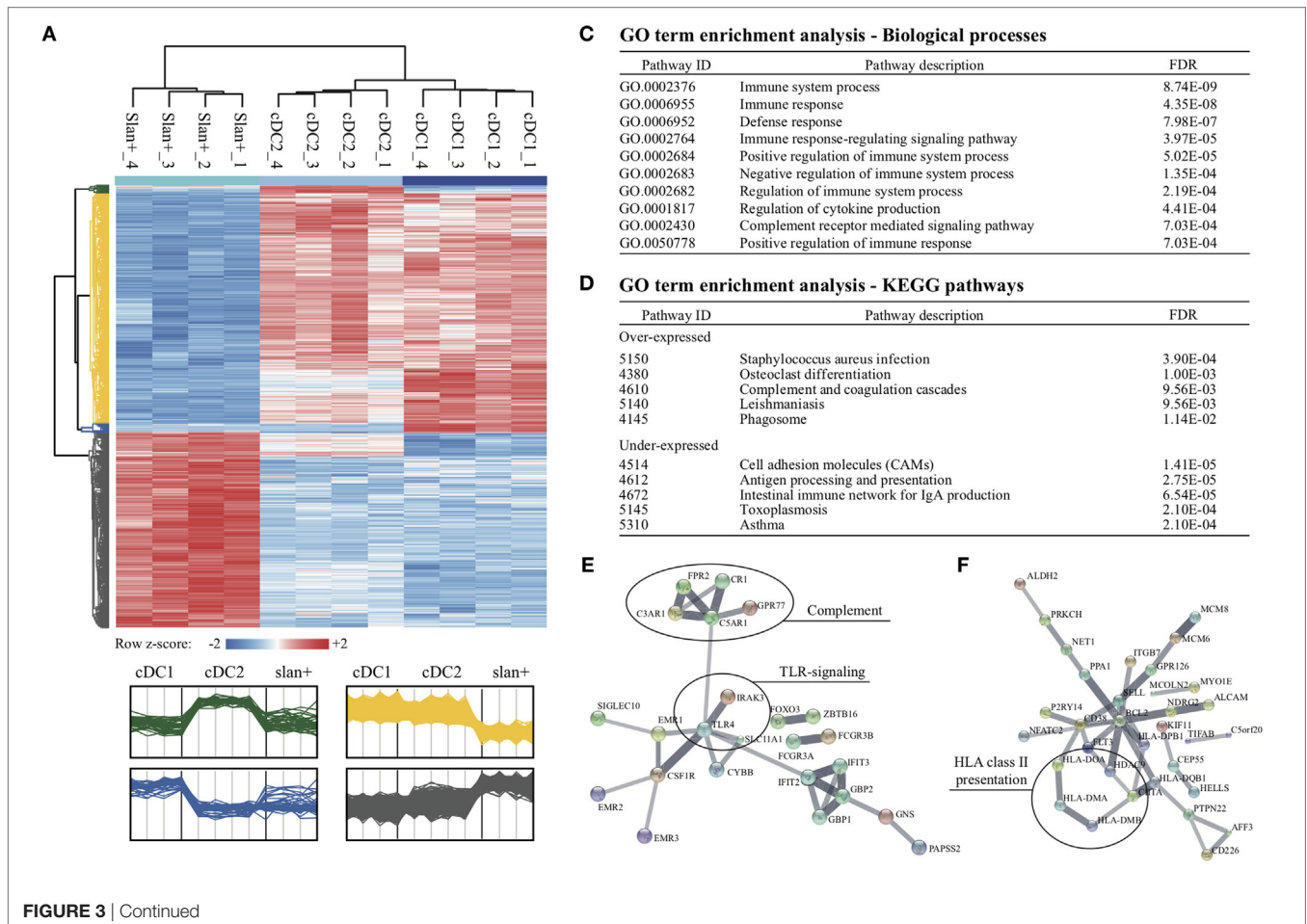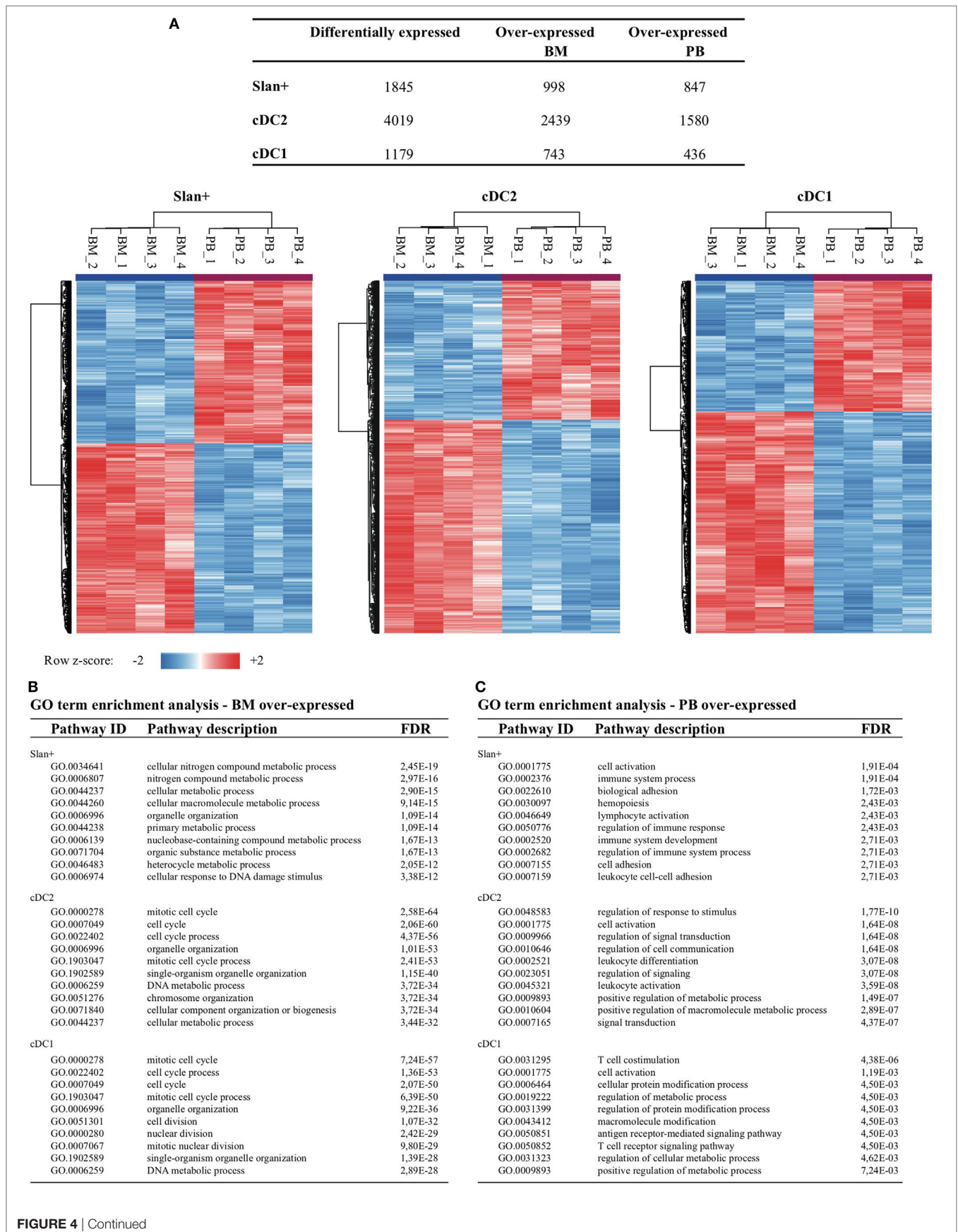

FIGURE 3 | Continued

B

Slan+ - Over-expressed

(Heatmap MEAN expression columns for Slan+ BM, cDC2 BM, cDC1 BM are color-coded, 1 = low to 10 = high.)

Probe Set ID	Gene Symbol	MEAN FC value	q-value Slan vs cDC1	q-value Slan vs cDC2
TC01006307.hg.1	FCGR3A	52.27	0.001	0.000
TC09000676.hg.1	C5AR1	42.83	0.001	0.002
TC11000821.hg.1	---	26.97	0.001	0.001
TC14000698.hg.1	---	26.02	0.001	0.003
TC20000401.hg.1	LOC100506115	25.21	0.001	0.001
TC08001820.hg.1	TCF7L2	25.16	0.001	0.000
TC04001598.hg.1	LOC100507639	24.82	0.002	0.003
TC12001171.hg.1	C3AR1	22.74	0.002	0.004
TC01001602.hg.1	MTSS1	22.26	0.000	0.000
TC15001441.hg.1	DMXL2	17.03	0.001	0.002
TC19000120.hg.1	EMR1	14.03	0.002	0.003
TCl1003451.hg.1	MS4A7	13.84	0.005	0.003
TC01006308.hg.1	FCGR3B	13.75	0.002	0.002
TC01006361.hg.1	GBP2	13.74	0.002	0.002
TC02000192.hg.1	CLIP4	11.76	0.002	0.001
TC10000629.hg.1	LIPN	11.30	0.002	0.009
TC01000677.hg.1	C5AR2	10.54	0.003	0.003
TC01003458.hg.1	SH2D1B	10.39	0.037	0.041
TC11002308.hg.1	---	9.98	0.003	0.003
TC0X000171.hg.1	CYBB	9.67	0.030	0.016
TC19000788.hg.1	FPR2	9.67	0.000	0.001
TC03000526.hg.1	LOC152225	9.30	0.002	0.002
TC14000936.hg.1	SLC7A7	8.72	0.001	0.001
TC01001842.hg.1	LILRB2	8.40	0.001	0.001
TC12000591.hg.1	IRAK3	7.95	0.029	0.027
TC15000407.hg.1	---	7.94	0.001	0.002
TC08000516.hg.1	OTTHUMG00000164594	7.91	0.005	0.003
TC07001002.hg.1	GIMAP8	7.82	0.009	0.021
TC14001466.hg.1	SIRPONA1	7.82	0.000	0.002
TC15000021.hg.1	REREP3	7.70	0.010	0.003
TC19001241.hg.1	EMR3	7.69	0.004	0.006
TC09000601.hg.1	TLR4	7.68	0.003	0.008
TC07003314.hg.1	PILRA	7.64	0.001	0.003
TC06001853.hg.1	OTTHUMG00000014981	7.59	0.014	0.013
TC07001618.hg.1	PDK4	7.59	0.003	0.036
TC08000515.hg.1	OTTHUMG00000164593	7.57	0.010	0.011
TC02000909.hg.1	---	7.53	0.036	0.028
TC10000636.hg.1	IFIT2	7.41	0.044	0.003
TC15000441.hg.1	AQP9	7.34	0.002	0.003
TC20000844.hg.1	MAFB	7.25	0.001	0.002
TC01002849.hg.1	GBP4	7.24	0.001	0.004
TC05001932.hg.1	CSF1R	7.23	0.001	0.005
TC01003996.hg.1	LYST	7.21	0.011	0.026
TC01002850.hg.1	GBP5	7.19	0.002	0.002
TC02001696.hg.1	BRE-AS1	6.99	0.011	0.015
TC03001304.hg.1	CX3CR1	6.92	0.014	0.014
TC09000400.hg.1	CTSL1	6.78	0.001	0.000
TC17000396.hg.1	SLFN5	6.77	0.003	0.004
TC17001725.hg.1	CHST15	6.74	0.004	0.002
TC19001242.hg.1	EMR2	6.50	0.003	0.002
TC03000836.hg.1	OTTHUMG00000159695	6.25	0.005	0.009
TC04000469.hg.1	PTPN13	6.12	0.004	0.011
TC19000180.hg.1	SLC44A2	6.11	0.010	0.001
TC01000834.hg.1	OTTHUMG00000010124	6.08	0.003	0.004
TC14000433.hg.1	SIPA1L1	5.88	0.002	0.003
TC10001669.hg.1	OTTHUMG00000019066	5.62	0.003	0.003
TC11002247.hg.1	CASP5	5.61	0.018	0.025
TC01002847.hg.1	GBP1	5.60	0.001	0.031
TC06000950.hg.1	SMPDL3A	5.56	0.009	0.009
TC00000798.hg.1	PTP4A3	5.53	0.001	0.001
TC14000691.hg.1	SNORD114-14	5.50	0.016	0.017
TC04002955.hg.1	ARAP2	5.49	0.007	0.004
TC02001300.hg.1	SLC11A1	5.49	0.000	0.000
TC19001293.hg.1	ZCCHC6	5.48	0.001	0.001
TC17001798.hg.1	PECAM1	5.43	0.002	0.001
TC01001581.hg.1	NPL	5.39	0.001	0.001
TC15000408.hg.1	---	5.32	0.001	0.002
TC02002399.hg.1	ZEB2	5.27	0.029	0.014
TC08001120.hg.1	RNF122	5.24	0.014	0.004
TC08001550.hg.1	---	5.05	0.010	0.009
TC03001720.hg.1	HEG1	5.03	0.004	0.006
TC10000637.hg.1	IFIT3	4.98	0.008	0.046
TC08001361.hg.1	PAG1	4.98	0.005	0.003
TC14000676.hg.1	SNORD114-1	4.94	0.007	0.009
TC12001678.hg.1	GNS	4.90	0.002	0.008
TC01001504.hg.1	CH25H	4.77	0.003	0.012
TC19002653.hg.1	LILRA1	4.73	0.017	0.008
TC08001015.hg.1	ASAH1	4.72	0.004	0.010
TC05000226.hg.1	SNX18	4.72	0.030	0.011
TC11001048.hg.1	SIDT2	4.69	0.005	0.003
TC05001295.hg.1	FYB	4.68	0.011	0.018
TC14000645.hg.1	MIG3	4.66	0.010	0.011
TC11003452.hg.1	MS4A14	4.57	0.005	0.010
TC09001204.hg.1	TMEM2	4.56	0.000	0.001
TC15000259.hg.1	SPRED1	4.56	0.013	0.005
TC03001071.hg.1	HES1	4.55	0.003	0.018
TC11001026.hg.1	ZBTBl6	4.54	0.002	0.001
TC14002503.hg.1	FLVCR2	4.52	0.009	0.021
TC06000868.hg.1	FOXO3	4.42	0.004	0.005
TC19002654.hg.1	LILRBl	4.40	0.006	0.003
TC19001779.hg.1	SIGLEC10	4.40	0.018	0.001
TC01001738.hg.1	CRl	4.38	0.003	0.007
TC19001287.hg.1	LRRC25	4.32	0.021	0.010
TC06000621.hg.1	PAPSS2	4.18	0.010	0.008
TC19002615.hg.1	LILRA3	4.18	0.003	0.005
TC16000211.hg.1	SYT17	4.16	0.007	0.008
TC08000517.hg.1	OTTHUMG00000164595	4.15	0.013	0.017
TC12001796.hg.1	DUSP6	4.14	0.006	0.013
TC17001979.hg.1	SECTM1	4.12	0.002	0.002
TC05002051.hg.1	LOC100128059	4.11	0.018	0.002

cDC2 - Over-expressed

Probe Set ID	Gene Symbol	MEAN FC value	q-value cDC2 vs Slan	q-value cDC2 vs cDC1
TC01001339.hg.1	CD1C	40.70	0.000	0.015
TC05000412.hg.1	VCAN	14.43	0.002	0.029
TC05001556.hg.1	VCAN-AS1	13.99	0.008	0.049
TC12001162.hg.1	CD163	13.73	0.000	0.033
TC10000135.hg.1	MRC1	6.25	0.010	0.049
TC15001183.hg.1	FMN1	5.66	0.001	0.039
TC01001340.hg.1	CD1E	4.82	0.007	0.047
TC14000359.hg.1	---	4.18	0.014	0.015
TC18000141.hg.1	DTNA	3.20	0.000	0.041
TC12001269.hg.1	PLBD1	3.20	0.007	0.015
TC07000735.hg.1	CPED1	2.80	0.038	0.050
TC10001136.hg.1	MPP7	2.41	0.004	0.039
TC16000473.hg.1	MT1F	2.22	0.037	0.039
TC07001768.hg.1	LOC401397	2.10	0.003	0.045
TC14001182.hg.1	RTN1	2.09	0.005	0.044
TC01002512.hg.1	CSF3R	2.03	0.007	0.043
TC03001540.hg.1	FRMD4B	2.02	0.002	0.036
TC16000476.hg.1	MT1X	1.98	0.024	0.033
TC07000178.hg.1	CREB5	1.95	0.003	0.039
TC10000488.hg.1	C10orf11	1.84	0.019	0.045
TC02000626.hg.1	OTTHUMG00000153092	1.76	0.006	0.046
TC11001124.hg.1	GRAMD1B	1.65	0.010	0.029
TC11000027.hg.1	TALDO1	1.56	0.004	0.029
TC06001773.hg.1	PLA2G7	1.33	0.009	0.029
TC12000531.hg.1	MARS	1.33	0.005	0.046

cDC1 - Over-expressed

Probe Set ID	Gene Symbol	MEAN FC value	q-value cDC1 vs cDC2	q-value cDC1 vs Slan
TC06000985.hg.1	ENPP1	21.20	0.033	0.004
TC04001036.hg.1	CLNK	19.84	0.015	0.001
TCl1002316.hg.1	CADM1	18.56	0.015	0.001
TC03001646.hg.1	GCSAM	12.93	0.029	0.001
TC08001248.hg.1	TOX	12.89	0.039	0.002
TC03001354.hg.1	XCR1	12.40	0.033	0.004
TC12001556.hg.1	CLEC9A	11.99	0.033	0.003
TC01001182.hg.1	C1orf54	11.49	0.031	0.001
TC12001269.hg.1	OTTHUMG00000018181	11.37	0.045	0.002
TC10000323.hg.1	WDFY4	10.74	0.031	0.002
TC14001451.hg.1	LGMN	10.40	0.033	0.000
TC11001033.hg.1	---	10.22	0.039	0.009
TC10000324.hg.1	OTTHUMG00000018179	9.54	0.033	0.007
TC02002478.hg.1	DPP4	9.33	0.015	0.001
TC05000378.hg.1	OTTHUMG00000162471	7.21	0.042	0.002
TC6_mcf_hap5000224.hg.1	HLA-DOB	6.85	0.039	0.002
TC01001372.hg.1	SLAMF7	6.62	0.007	0.029
TC13000644.hg.1	KIAA0226L	6.22	0.031	0.004
TC04001486.hg.1	CAMK2D	6.17	0.033	0.003
TC06000458.hg.1	---	5.77	0.042	0.004
TC01001357.hg.1	SLAMF8	5.49	0.033	0.002
TC10000219.hg.1	ZEB1	5.30	0.039	0.001
TC11001034.hg.1	---	5.26	0.046	0.008
TC08000539.hg.1	CPNE3	5.22	0.036	0.006
TC03000213.hg.1	OTTHUMG00000156011	4.89	0.043	0.014
TC14001022.hg.1	EGLN3	4.74	0.029	0.001
TC16000666.hg.1	IRF8	4.32	0.029	0.001
TC14000397.hg.1	FUT8	4.28	0.039	0.004
TC16001240.hg.1	VAC14	4.13	0.047	0.007
TC22000350.hg.1	SEPT3	3.85	0.015	0.000
TC21000344.hg.1	CYYR1	3.72	0.036	0.006
TC03000375.hg.1	FLNB	3.39	0.041	0.009
TC01003759.hg.1	C1orf186	3.08	0.046	0.008
TC03000607.hg.1	ARHGAP31	2.86	0.043	0.002
TC15001257.hg.1	EHD4	2.84	0.039	0.003
TC08000220.hg.1	FZD3	2.83	0.046	0.002
TC04000570.hg.1	SLC24A4	2.83	0.031	0.009
TC18000221.hg.1	TNFRSF11A	2.74	0.036	0.002
TC05001986.hg.1	ADAM19	2.57	0.038	0.001
TC09001656.hg.1	FNBP1	2.57	0.039	0.008
TC09000567.hg.1	KIAA1958	2.34	0.033	0.002
TC10002352.hg.1	FUCA1	2.33	0.049	0.023
TC05000096.hg.1	BASP1	2.13	0.045	0.001
TC01006276.hg.1	PPM1J	2.06	0.015	0.004
TC01001356.hg.1	FCRL6	2.05	0.039	0.004
TC6_apd_hap1000130.hg.1	TAP2	1.91	0.039	0.020
TC0X001020.hg.1	PIM2	1.84	0.033	0.012
TC03002106.hg.1	LEPREL1	1.80	0.039	0.002
TC05000682.hg.1	TGFBI	1.76	0.039	0.040
TCl1002074.hg.1	UCP2	1.75	0.031	0.006
TC09001618.hg.1	FAM102A	1.73	0.039	0.005
TC20000819.hg.1	SOGA1	1.57	0.028	0.001
TC01001989.hg.1	DISI2	1.55	0.039	0.010
TC07003292.hg.1	LSMEM1	1.54	0.045	0.044
TC07001885.hg.1	WDR91	1.51	0.038	0.019
TC09000550.hg.1	AKAP2	1.46	0.033	0.003
TC10001420.hg.1	CAMK2G	1.40	0.034	0.003
TC19001635.hg.1	SYMPK	1.35	0.029	0.002
TC19000118.hg.1	TRIP10	1.28	0.046	0.018
TC06001123.hg.1	ARID1B	1.21	0.033	0.028

Expression level: 1   10

FIGURE 3 | Differentially expressed genes (DEGs) between slan+ monocytes and cDC2 and cDC1 in the bone marrow (BM) compartment. After identification, DEGs were further analyzed for the three cell subsets in the BM compartment. **(A)** Cluster analysis of transcripts that are differentially expressed between the subsets are presented in a heat map. Each row represents a single transcript. Relative expression levels for four donors per subset are shown. z-scores were calculated in one row to show the relative expression values per donor compared to the mean of the entire row (z-score −2: low expression, z-score +2: high expression). Four different clusters were generated. In green, DEGs that were over-expressed in cDC2 are shown, whereas DEGs over-expressed in cDC1 are within the blue cluster. Under- and over-expressed transcripts for slan+ monocytes are shown in yellow and gray, respectively. **(B)** Coding and over-expressed transcripts, sorted on mean FC values, are shown for all cell subsets. For slan+ monocytes the top 100 is used, whereas for the other two cell subsets 25 and 60 transcripts are shown (cDC2 and cDC1, respectively). For each transcript, the mean absolute expression level of four donors (1: low expression, 10: high expression) is color coded in the given cell subset. Q-values for both comparisons (i.e., slan+ vs cDC2 and slan+ vs cDC1) are shown. **(C)** Pathway analysis of over-expressed transcripts in slan+ monocytes compared to both DC subsets. The top 100 highest FC values from over-expressed coding transcripts were imported into the STRING v10.0 bioinformatics tool and significant enriched pathways were identified. From this list, the top 10 with lowest FDR (out of 62) of enriched biological processes are shown. **(D)** Enriched KEGG pathways for over- and under-expressed transcripts in slan+ monocytes compared to DC subsets. Top 100 highest FC values of coding transcripts were used from the over- and under-expressed gene lists. An interaction network analysis of involved transcripts is displayed for over-expressed genes **(E)** as well as for under-expressed genes **(F)** in slan+ monocytes. Disconnected nodes are hidden and the line thickness indicates the strength of data support. Abbreviations: FC, fold change; FDR, false discovery rate; GO, gene ontology; ID, identification; KEGG, Kyoto encyclopedia of genes and genomes.

described CD1c+ (cDC2) and CD141+ (cDC1) myeloid DC subsets. These two subsets have been widely studied in a healthy and diseased context, in PB and secondary lymphoid organs such as tonsils, lymph nodes, and spleen (35, 41–44). Their exact developmental state and immunological role in the human BM compartment, however, have not been explored before. Therefore,

A

	Differentially expressed	Over-expressed BM	Over-expressed PB
Slan+	1845	998	847
cDC2	4019	2439	1580
cDC1	1179	743	436

Row z-score: −2   +2

B

GO term enrichment analysis - BM over-expressed

Pathway ID	Pathway description	FDR
Slan+		
GO.0034641	cellular nitrogen compound metabolic process	2,45E-19
GO.0006807	nitrogen compound metabolic process	2,97E-16
GO.0044237	cellular metabolic process	2,90E-15
GO.0044260	cellular macromolecule metabolic process	9,14E-15
GO.0006996	organelle organization	1,09E-14
GO.0044238	primary metabolic process	1,09E-14
GO.0006139	nucleobase-containing compound metabolic process	1,67E-13
GO.0071704	organic substance metabolic process	1,67E-13
GO.0046483	heterocycle metabolic process	2,05E-12
GO.0006974	cellular response to DNA damage stimulus	3,38E-12
cDC2		
GO.0000278	mitotic cell cycle	2,58E-64
GO.0007049	cell cycle	2,06E-60
GO.0022402	cell cycle process	4,37E-56
GO.0006996	organelle organization	1,01E-53
GO.1903047	mitotic cell cycle process	2,41E-53
GO.1902589	single-organism organelle organization	1,15E-40
GO.0006259	DNA metabolic process	3,72E-34
GO.0051276	chromosome organization	3,72E-34
GO.0071840	cellular component organization or biogenesis	3,72E-34
GO.0044237	cellular metabolic process	3,44E-32
cDC1		
GO.0000278	mitotic cell cycle	7,24E-57
GO.0022402	cell cycle process	1,36E-53
GO.0007049	cell cycle	2,07E-50
GO.1903047	mitotic cell cycle process	6,39E-50
GO.0006996	organelle organization	9,22E-36
GO.0051301	cell division	1,07E-32
GO.0000280	nuclear division	2,42E-29
GO.0007067	mitotic nuclear division	9,80E-29
GO.1902589	single-organism organelle organization	1,39E-28
GO.0006259	DNA metabolic process	2,89E-28

C

GO term enrichment analysis - PB over-expressed

Pathway ID	Pathway description	FDR
Slan+		
GO.0001775	cell activation	1,91E-04
GO.0002376	immune system process	1,91E-04
GO.0022610	biological adhesion	1,72E-03
GO.0030097	hemopoiesis	2,43E-03
GO.0046649	lymphocyte activation	2,43E-03
GO.0050776	regulation of immune response	2,43E-03
GO.0002520	immune system development	2,71E-03
GO.0002682	regulation of immune system process	2,71E-03
GO.0007155	cell adhesion	2,71E-03
GO.0007159	leukocyte cell-cell adhesion	2,71E-03
cDC2		
GO.0048583	regulation of response to stimulus	1,77E-10
GO.0001775	cell activation	1,64E-08
GO.0009966	regulation of signal transduction	1,64E-08
GO.0010646	regulation of cell communication	1,64E-08
GO.0002521	leukocyte differentiation	3,07E-08
GO.0023051	regulation of signaling	3,07E-08
GO.0045321	leukocyte activation	3,59E-08
GO.0009893	positive regulation of metabolic process	1,49E-07
GO.0010604	positive regulation of macromolecule metabolic process	2,89E-07
GO.0007165	signal transduction	4,37E-07
cDC1		
GO.0031295	T cell costimulation	4,38E-06
GO.0001775	cell activation	1,19E-03
GO.0006464	cellular protein modification process	4,50E-03
GO.0019222	regulation of metabolic process	4,50E-03
GO.0031399	regulation of protein modification process	4,50E-03
GO.0043412	macromolecule modification	4,50E-03
GO.0050851	antigen receptor-mediated signaling pathway	4,50E-03
GO.0050852	T cell receptor signaling pathway	4,50E-03
GO.0031323	regulation of cellular metabolic process	4,62E-03
GO.0009893	positive regulation of metabolic process	7,24E-03

FIGURE 4 | Continued

D

Gene Set Enrichment Analysis - enriched in bone marrow

KEGG pathway	Size	Matches	NES	q-value
KEGG_CELL_CYCLE	128	120	325.481	0.000
KEGG_DNA_REPLICATION	36	36	320.894	0.000
KEGG_NUCLEOTIDE_EXCISION_REPAIR	44	42	302.587	0.000
KEGG_PROTEASOME	48	43	295.279	0.000
KEGG_PYRIMIDINE_METABOLISM	98	90	292.316	0.000
KEGG_AMINOACYL_TRNA_BIOSYNTHESIS	41	41	289.418	0.000
KEGG_MISMATCH_REPAIR	23	23	287.716	0.000
KEGG_HOMOLOGOUS_RECOMBINATION	28	27	283.932	0.000
KEGG_RNA_DEGRADATION	59	58	281.599	0.000
KEGG_OOCYTE_MEIOSIS	114	107	266.693	0.000

Gene Set Enrichment Analysis - enriched in peripheral blood

KEGG pathway	Size	Matches	NES	q-value
KEGG_NEUROACTIVE_LIGAND_RECEPTOR_INTERACTION	272	265	243.252	0.000
KEGG_GRAFT_VERSUS_HOST_DISEASE	42	38	226.672	0.000
KEGG_ECM_RECEPTOR_INTERACTION	84	80	223.923	0.000
KEGG_CYTOKINE_CYTOKINE_RECEPTOR_INTERACTION	267	246	207.924	0.001
KEGG_HEMATOPOIETIC_CELL_LINEAGE	88	84	205.751	0.001
KEGG_TYPE_I_DIABETES_MELLITUS	44	41	204.326	0.001
KEGG_COMPLEMENT_AND_COAGULATION_CASCADES	69	69	204.294	0.001
KEGG_CELL_ADHESION_MOLECULES_CAMS	134	130	202.811	0.001
KEGG_ANTIGEN_PROCESSING_AND_PRESENTATION	89	79	200.844	0.001
KEGG_ARRHYTHMOGENIC_RIGHT_VENTRICULAR_CARDIOMYOPATHY_ARVC	76	73	200.228	0.001
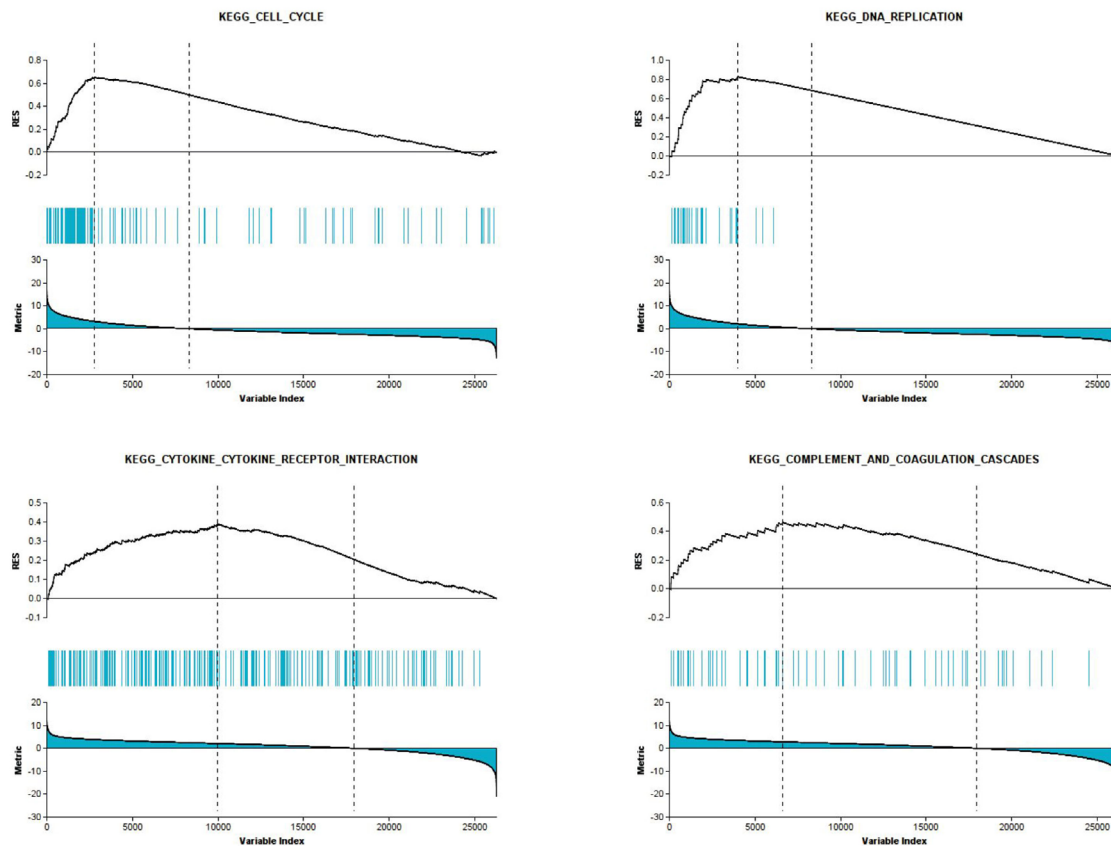
FIGURE 4 | Continued

FIGURE 4 | Transcriptomic comparison between cell subsets of the bone marrow (BM) vs the peripheral blood (PB) compartment. Gene expression profiles were compared between the BM and PB for each individual cell subset. **(A)** Number of differentially expressed transcripts found between the two different compartments (e.g., slan+ in BM vs slan+ in PB). Differentially expressed genes (DEGs) were clustered per row by using z-scores for each transcript, thereby reflecting relative expression levels. Heat maps for each individual subset are shown. For each cell subset, a pathway enrichment analysis was performed in which all DEGs were used that were over-expressed in BM **(B)** or over-expressed in PB **(C)**. Top 10 enriched biological processes for both compartments and each individual subset are shown. **(D)** Gene set enrichment analysis for BM- and PB-derived cell subsets. The top 10 of enriched KEGG pathways are shown together with four selected enrichment plots. Abbreviations: FDR, false discovery rate; GO, gene ontology; ID, identification; NES, normalized enrichment score.

FIGURE 5 | Continued

B cDC2   cDC1

1858 (71.4 %) | 581 (22.3 %) | 162 (6.2 %)

Overlapping genes over-expressed in BM

C cDC2   cDC1

1449 (76.9%) | 131 (6.9%) | 305 (16.2%)

Overlapping genes over-expressed in PB

D
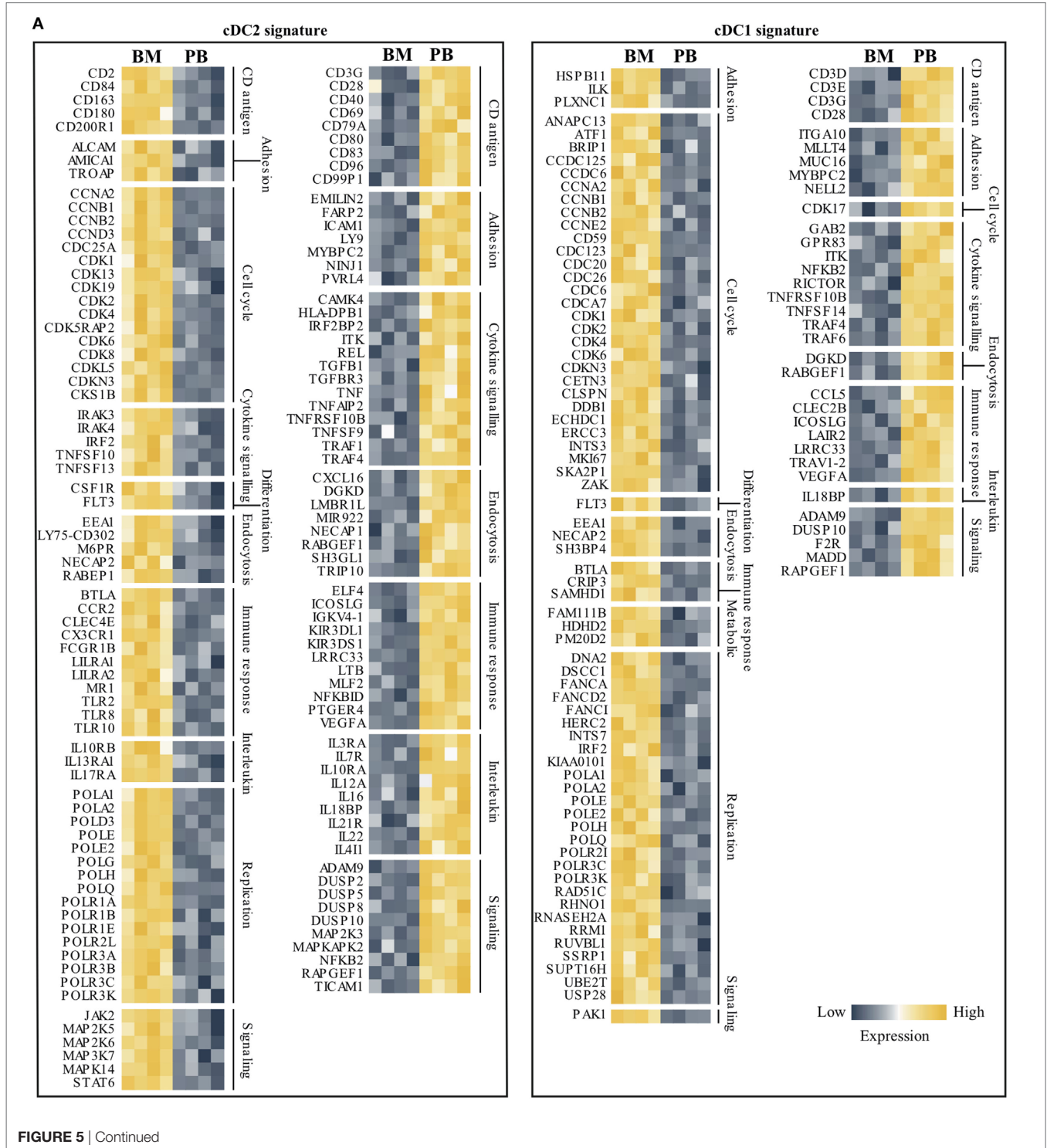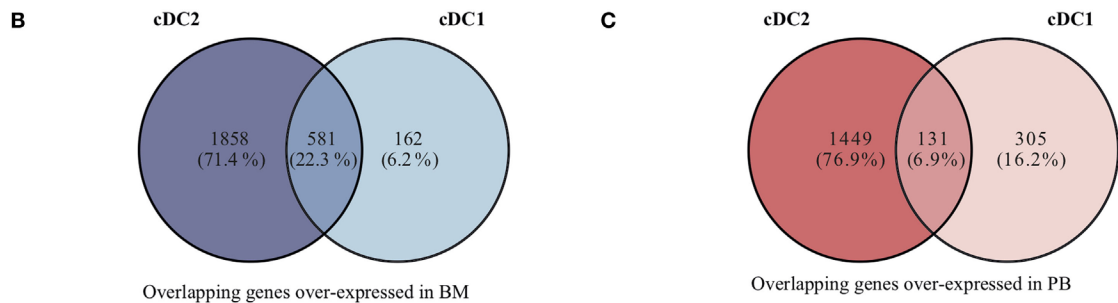
Biological process (GO)

Pathway ID	Pathway description	FDR
GO.0000278	mitotic cell cycle	1,66E-52
GO.0022402	cell cycle process	5,91E-50
GO.0007049	cell cycle	8,37E-48
GO.1903047	mitotic cell cycle process	1,80E-45
GO.0006996	organelle organization	4,07E-35
GO.0051301	cell division	7,68E-32
GO.1902589	single-organism organelle organization	2,44E-28
GO.0000280	nuclear division	3,56E-26
GO.0044770	cell cycle phase transition	4,77E-26
GO.0044772	mitotic cell cycle phase transition	2,15E-25

E

Biological process (GO)

Pathway ID	Pathway description	FDR
GO.0006950	response to stress	8,27E-04
GO.0031295	T cell costimulation	8,27E-04
GO.0001775	cell activation	2,89E-03
GO.0030154	cell differentiation	3,81E-03
GO.0043304	regulation of mast cell degranulation	1,00E-02
GO.0050851	antigen receptor-mediated signaling pathway	1,00E-02
GO.0008152	metabolic process	1,08E-02
GO.0033554	cellular response to stress	1,08E-02
GO.0048534	hematopoietic or lymphoid organ development	1,25E-02
GO.2000177	regulation of neural precursor cell proliferation	1,25E-02

F
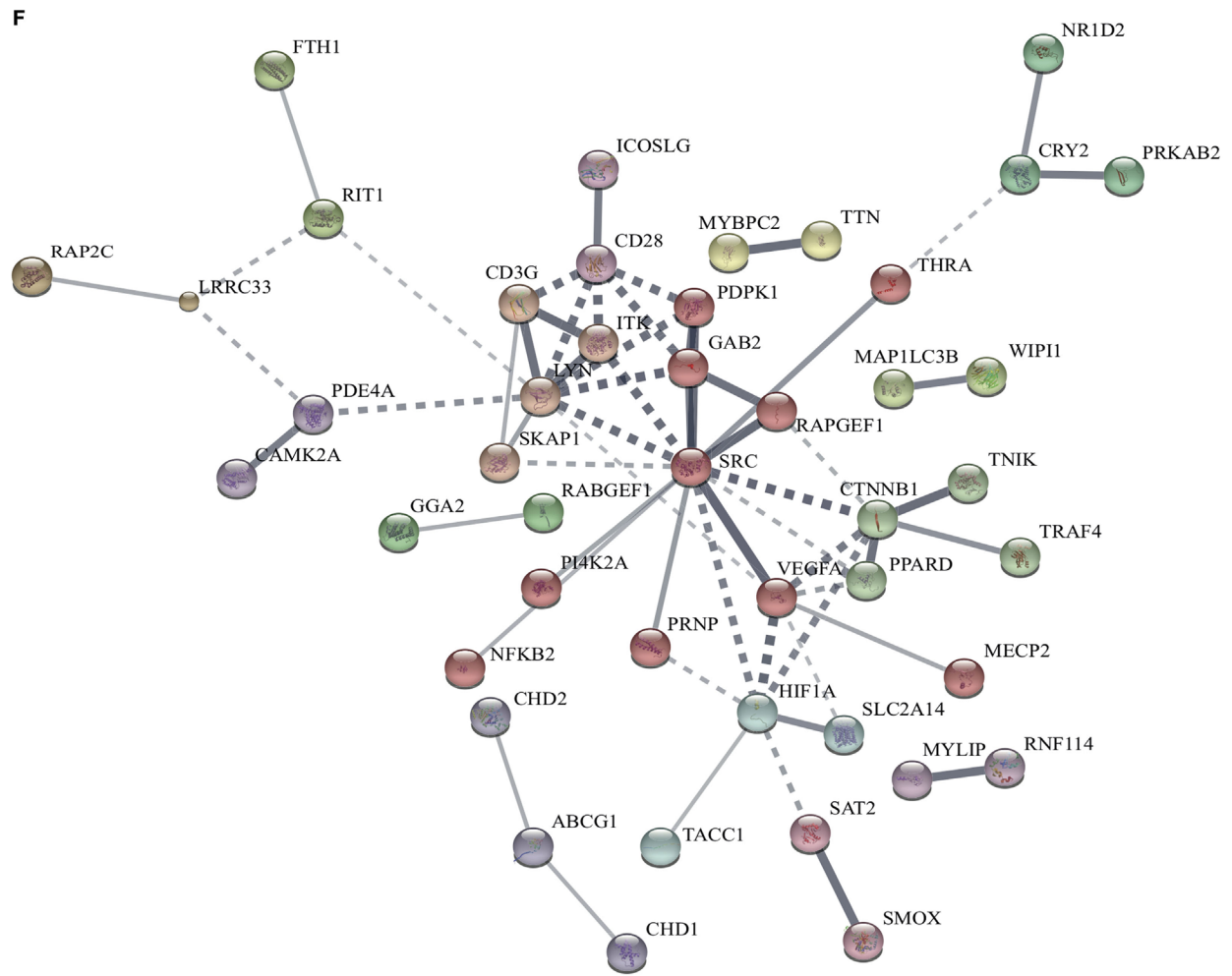
FIGURE 5 | Continued

FIGURE 5 | Compartment-specific DC gene signatures for cDC2 and cDC1. Both myeloid DC subsets were further analyzed to find compartment-specific DC gene signatures. **(A)** Transcripts were filtered based on gene descriptions and GO biological process terms by using cell cycle- and immune response-related terms. Relative expression for cDC2 and cDC1 in both bone marrow (BM) as well as peripheral blood (PB) are shown for selected genes. Venn diagrams were used to obtain overlapping genes between cDC2 and cDC1 in the BM **(B)** and PB **(C)** compartment. **(D)** The 581 commonly over-expressed transcripts in BM-derived DCs were used in a pathway enrichment analysis. **(E)** Similarly, overlapping transcripts (131 in total) of PB cDC2 and cDC21 were used in the STRING pathway analysis. **(F)** An interaction network of the PB transcripts was generated. In total, 85 genes could be annotated. The minimum required interaction score was set to medium confidence (0.400), disconnected nodes were hidden and the thickness of the lines indicates the strength of data support. Abbreviations: FDR, false discovery rate; GO, gene ontology; ID, identification.
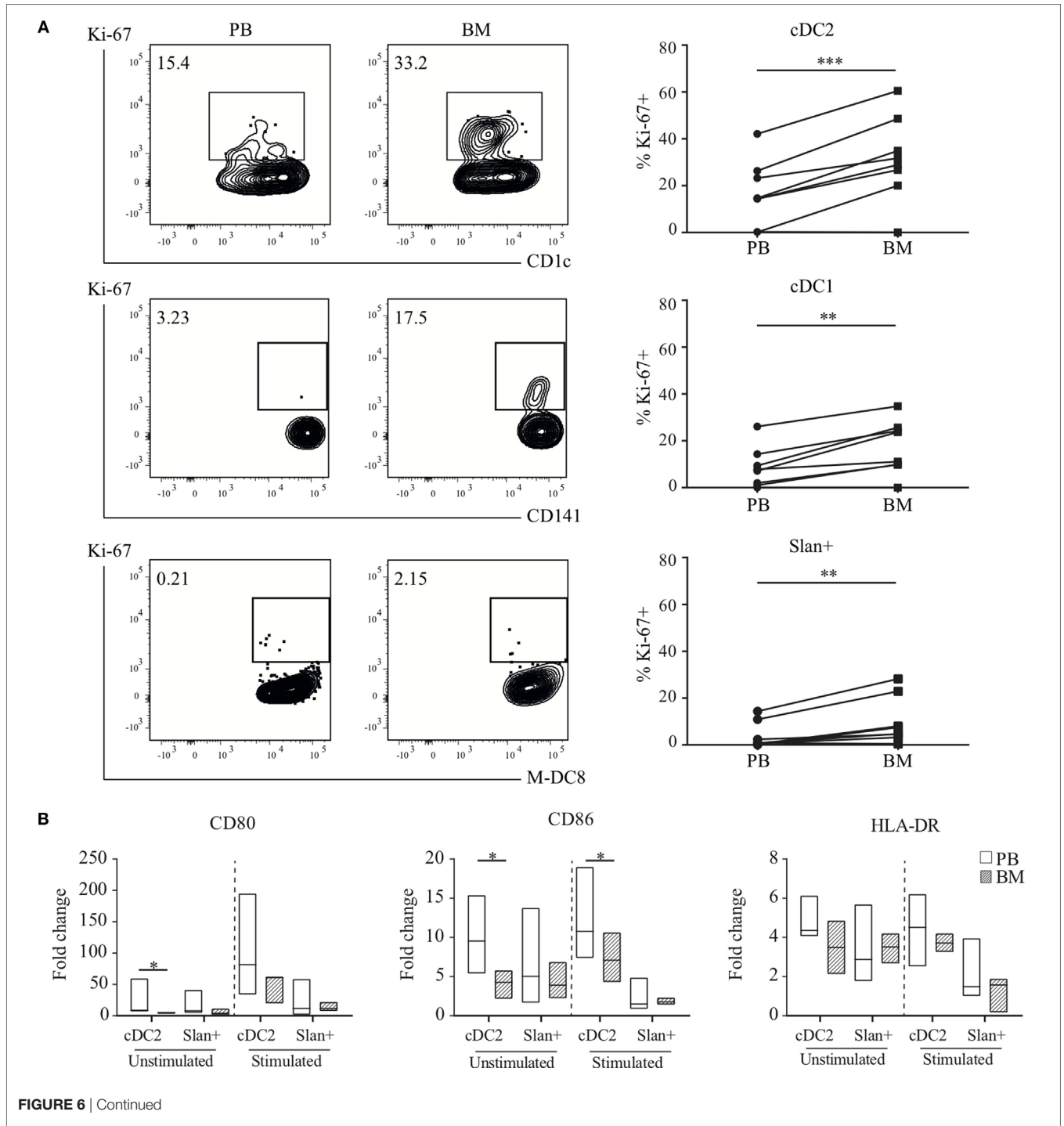
FIGURE 6 | Continued
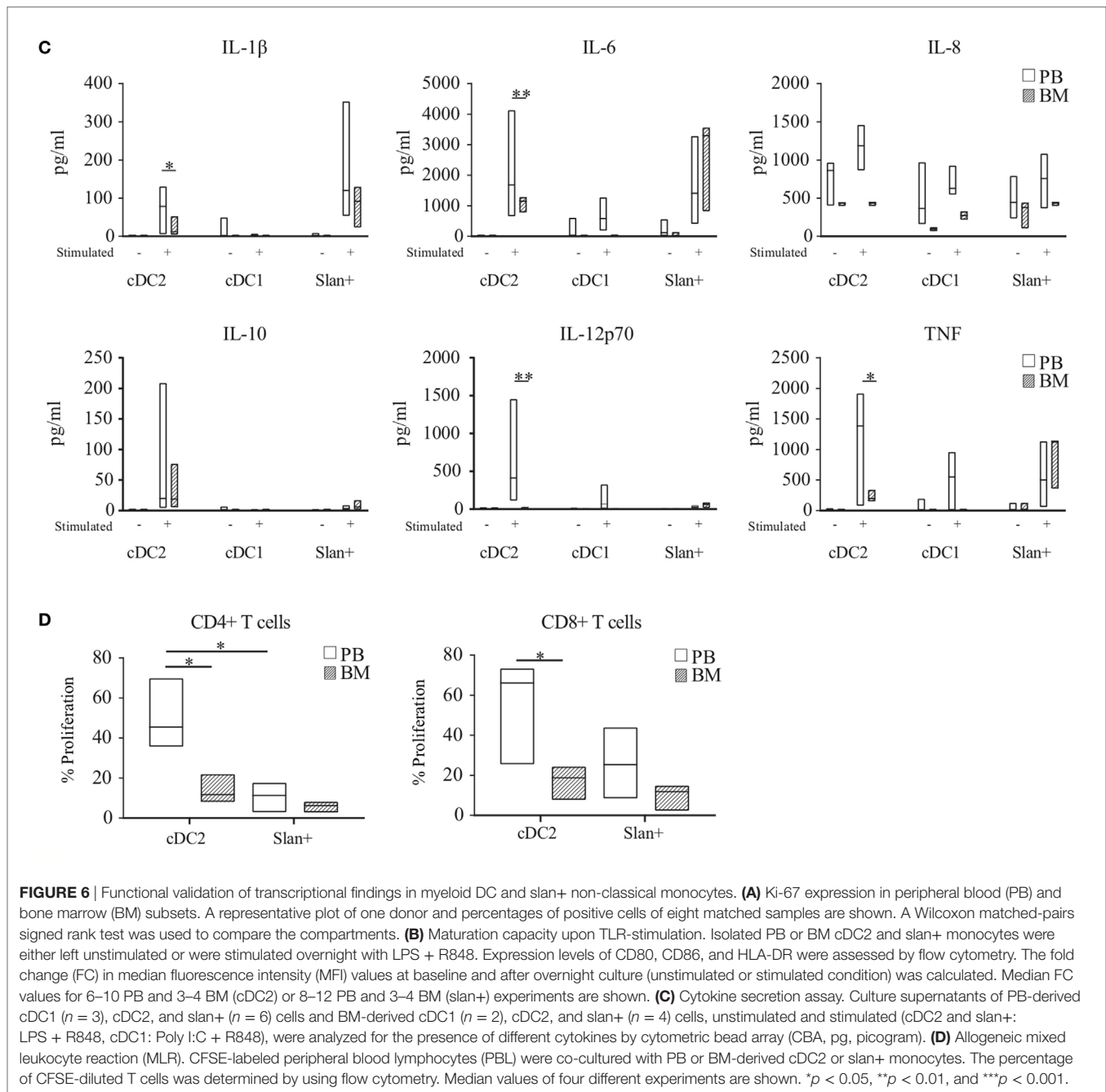
FIGURE 6 | Functional validation of transcriptional findings in myeloid DC and slan+ non-classical monocytes. **(A)** Ki-67 expression in peripheral blood (PB) and bone marrow (BM) subsets. A representative plot of one donor and percentages of positive cells of eight matched samples are shown. A Wilcoxon matched-pairs signed rank test was used to compare the compartments. **(B)** Maturation capacity upon TLR-stimulation. Isolated PB or BM cDC2 and slan+ monocytes were either left unstimulated or were stimulated overnight with LPS + R848. Expression levels of CD80, CD86, and HLA-DR were assessed by flow cytometry. The fold change (FC) in median fluorescence intensity (MFI) values at baseline and after overnight culture (unstimulated or stimulated condition) was calculated. Median FC values for 6–10 PB and 3–4 BM (cDC2) or 8–12 PB and 3–4 BM (slan+) experiments are shown. **(C)** Cytokine secretion assay. Culture supernatants of PB-derived cDC1 ($n = 3$), cDC2, and slan+ ($n = 6$) cells and BM-derived cDC1 ($n = 2$), cDC2, and slan+ ($n = 4$) cells, unstimulated and stimulated (cDC2 and slan+: LPS + R848, cDC1: Poly I:C + R848), were analyzed for the presence of different cytokines by cytometric bead array (CBA, pg, picogram). **(D)** Allogeneic mixed leukocyte reaction (MLR). CFSE-labeled peripheral blood lymphocytes (PBL) were co-cultured with PB or BM-derived cDC2 or slan+ monocytes. The percentage of CFSE-diluted T cells was determined by using flow cytometry. Median values of four different experiments are shown. *$p < 0.05$, **$p < 0.01$, and ***$p < 0.001$.

we carried out a genomic as well as a functional study in which we compared both DC subsets and the slan+ non-classical monocytes from BM to their PB counterparts.

The frequency of different subsets in the BM and PB already showed compartment-related differences. cDC1 were more frequent in the BM compartment than in the PB, whereas slan+ non-classical monocyte levels were clearly higher in PB compared to BM. Initially, slan+ non-classical monocytes were considered to belong to the DC lineage (38, 45), but recent insights firmly place them in the monocyte population (also confirmed in our previous study) (30, 32). The immunophenotypic analysis

performed in our current study also supports this reallocation for BM-derived slan+ non-classical monocytes. They showed significantly lower expression levels of HLA-DR as compared to the myeloid DC subsets and similar levels as compared to their PB counterparts and CD14+ classical monocytes. Additional evidence is provided by our transcriptional findings. BM-derived slan+ non-classical monocytes clearly clustered away from the cDC2 and cDC1 and showed the most distinct gene signature with the highest number of DEGs. These differentially expressed transcripts could be translated into pathways that were related to involvement in innate immune responses and a low capacity

for DC-like functionalities such as antigen processing and presentation, comparable to PB findings (30). For BM DC subsets, over-expressed genes confirmed their lineage commitment and a consistent subset-specific gene expression profile between PB and BM. However, beside these conserved transcripts, large differences in gene expression were found between the two compartments. In a hierarchical clustering, DC from one compartment clustered closer together than that they did with their equivalent in the other compartment, indicating a location-dependent transcriptional profile. Both cDC2 and cDC1 showed similar enrichment patterns in BM and PB. In BM, a network of cell cycle and differentiation transcripts was found to be over-expressed, whereas in PB, immune-related effector genes were overrepresented. The development of DC is highly dependent on Fms-related tyrosine kinase 3 ligand (46–48). Its receptor, Flt3 (CD135), is expressed in all stages, but highest levels can be found in the most immature forms. From our transcriptional data, both subsets showed over-expression of *FLT3* in the BM compartment, thereby supporting the hypothesis that BM-derived cDC2 and cDC1 are in a more immature and differentiating state than their PB equivalents. Validation of the transcriptional findings by evaluating the expression levels of the proliferation marker Ki-67, further confirmed the FLT3-responsive and proliferative state of BM DC as compared to PB DC. From a functional perspective, a similar conclusion can be drawn. DC from the BM compartment showed a lower activity in DC-like functionalities as compared to matched DC from PB. Upon TLR-triggering, using a known synergistic combination of LPS and R848, BM-derived cDC2 were less able to up-regulate co-stimulatory molecules (in particular CD80), which was reflected in their low capacity for T cell priming. The induction of CD4+ and CD8+ T cell proliferation was substantially lower for BM cDC2 than for PB cDC2. Additionally, the ability of BM DC to secrete pro-inflammatory cytokines was inferior to PB DC. In particular, the production of IL-12p70, a cytokine specifically secreted by highly specialized DC subsets, was nearly absent in BM subsets. For slan+ non-classical monocytes the differences between the two compartments was less evident. Their non-DC-like character was confirmed in both compartments, suggesting minimal effects of the location and a more stable and differentiated state of this cell type.

In conclusion, this study provides the first transcriptional and functional findings for myeloid DC subsets in the human BM. In this compartment, DC harbor more immature and less differentiated features and are not equipped yet to fully exert DC-like functions. These data reveal the BM primarily as a DC developmental location rather than an effector site. Slan+ non-classical monocytes, on the other hand, seem to enter the BM as effectors from the PB in accordance to their more differentiated state and patrolling immune function. In several BM-derived diseases, such as certain hematological malignancies, DC function, and frequency is disturbed potentially causing altered immune responses that may be involved in the pathogenesis of the disease. However, most of these studies focused on PB-derived DC, and only some studied the equivalent forms of DC in the BM compartment (49–57). Since disease development in these disorders probably arises in the BM compartment itself, it is of high interest to study altered immune processes in this compartment rather than only in the PB. Results from this study on healthy BM DC may thus serve as a baseline for further immunological research on aberrant DC function in such disorders.

ETHICS STATEMENT

The study was approved by the local ethical committee. All subjects gave written informed consent in accordance with the Declaration of Helsinki.

AUTHOR CONTRIBUTIONS

Contribution: NL-K and KL performed experiments and analyzed data. NL-K, KL, TW, HB, SK, TG, ML, and AL interpreted data. NL-K, KL, TG, ML, and AL designed research. NL-K wrote the paper.

SUPPLEMENTARY MATERIAL

The Supplementary Material for this article can be found online at https://www.frontiersin.org/articles/10.3389/fimmu.2018.01619/full#supplementary-material.

REFERENCES

1. Geissmann F, Manz MG, Jung S, Sieweke MH, Merad M, Ley K. Development of monocytes, macrophages, and dendritic cells. *Science* (2010) 327(5966):656–61. doi:10.1126/science.1178331
2. Merad M, Sathe P, Helft J, Miller J, Mortha A. The dendritic cell lineage: ontogeny and function of dendritic cells and their subsets in the steady state and the inflamed setting. *Annu Rev Immunol* (2013) 31:563–604. doi:10.1146/annurev-immunol-020711-074950
3. Fogg DK, Sibon C, Miled C, Jung S, Aucouturier P, Littman DR, et al. A clonogenic bone marrow progenitor specific for macrophages and dendritic cells. *Science* (2006) 311(5757):83–7. doi:10.1126/science.1117729
4. Onai N, Obata-Onai A, Schmid MA, Ohteki T, Jarrossay D, Manz MG. Identification of clonogenic common Flt3+M-CSFR+ plasmacytoid and conventional dendritic cell progenitors in mouse bone marrow. *Nat Immunol* (2007) 8(11):1207–16. doi:10.1038/ni1518
5. Naik SH, Sathe P, Park HY, Metcalf D, Proietto AI, Dakic A, et al. Development of plasmacytoid and conventional dendritic cell subtypes from single precursor cells derived in vitro and in vivo. *Nat Immunol* (2007) 8(11):1217–26. doi:10.1038/ni1522
6. Liu K, Victora GD, Schwickert TA, Guermonprez P, Meredith MM, Yao K, et al. In vivo analysis of dendritic cell development and homeostasis. *Science* (2009) 324(5925):392–7. doi:10.1126/science.1170540
7. Ginhoux F, Liu K, Helft J, Bogunovic M, Greter M, Hashimoto D, et al. The origin and development of nonlymphoid tissue CD103+ DCs. *J Exp Med* (2009) 206(13):3115–30. doi:10.1084/jem.20091756
8. Inaba K, Inaba M, Deguchi M, Hagi K, Yasumizu R, Ikehara S, et al. Granulocytes, macrophages, and dendritic cells arise from a common major histocompatibility complex class II-negative progenitor in mouse bone marrow. *Immunology* (1993) 90:3038–42.
9. Diao J, Winter E, Chen W, Cantin C, Cattral MS. Characterization of distinct conventional and plasmacytoid dendritic cell-committed precursors in murine bone marrow. *J Immunol* (2004) 173(3):1826–33. doi:10.4049/jimmunol.173.3.1826
10. Traver D, Akashi K, Manz M, Merad M, Miyamoto T, Engleman EG, et al. Development of CD8α-positive dendritic cells from a common myeloid

progenitor. *Science* (2000) 290(5499):2152–4. doi:10.1126/science.290.5499.2152

11. Manz MG, Traver D, Miyamoto T, Weissman IL, Akashi K. Dendritic cell potentials of early lymphoid and myeloid progenitors. *Blood* (2001) 97(11):3333–41. doi:10.1182/blood.V97.11.3333

12. Shortman K, Naik SH. Steady-state and inflammatory dendritic-cell development. *Nat Rev Immunol* (2007) 7(1):19–30. doi:10.1038/nri1996

13. Robbins SH, Walzer T, Dembélé D, Thibault C, Defays A, Bessou G, et al. Novel insights into the relationships between dendritic cell subsets in human and mouse revealed by genome-wide expression profiling. *Genome Biol* (2008) 9(1):R17. doi:10.1186/gb-2008-9-1-r17

14. Poulin LF, Salio M, Griessinger E, Anjos-Afonso F, Craciun L, Chen JL, et al. Characterization of human DNGR-1+ BDCA3+ leukocytes as putative equivalents of mouse CD8alpha+ dendritic cells. *J Exp Med* (2010) 207(6):1261–71. doi:10.1084/jem.20092618

15. Haniffa M, Shin A, Bigley V, McGovern N, Teo P, See P, et al. Human tissues contain CD141hi cross-presenting dendritic cells with functional homology to mouse CD103+ nonlymphoid dendritic cells. *Immunity* (2012) 37(1):60–73. doi:10.1016/j.immuni.2012.04.012

16. Jongbloed SL, Kassianos AJ, McDonald KJ, Clark GJ, Ju X, Angel CE, et al. Human CD141+ (BDCA-3)+ dendritic cells (DCs) represent a unique myeloid DC subset that cross-presents necrotic cell antigens. *J Exp Med* (2010) 207(6):1247–60. doi:10.1084/jem.20092140

17. Bachem A, Güttler S, Hartung E, Ebstein F, Schaefer M, Tannert A, et al. Superior antigen cross-presentation and XCR1 expression define human CD11c+CD141+ cells as homologues of mouse CD8+ dendritic cells. *J Exp Med* (2010) 207(6):1273–81. doi:10.1084/jem.20100348

18. Lee J, Breton G, Oliveira TY, Zhou YJ, Aljoufi A, Puhr S, et al. Restricted dendritic cell and monocyte progenitors in human cord blood and bone marrow. *J Exp Med* (2015) 212(3):385–99. doi:10.1084/jem.20141442

19. Breton G, Lee J, Zhou YJ, Schreiber JJ, Keler T, Puhr S, et al. Circulating precursors of human CD1c+ and CD141+ dendritic cells. *J Exp Med* (2015) 212(3):401–13. doi:10.1084/jem.20141441

20. Breton G, Zheng S, Valieris R, Tojal da Silva I, Satija R, Nussenzweig MC. Human dendritic cells (DCs) are derived from distinct circulating precursors that are precommitted to become CD1c+ or CD141+ DCs. *J Exp Med* (2016) 213(13):2861–70. doi:10.1084/jem.20161135

21. Doulatov S, Notta F, Eppert K, Nguyen LT, Ohashi PS, Dick JE. Revised map of the human progenitor hierarchy shows the origin of macrophages and dendritic cells in early lymphoid development. *Nat Immunol* (2010) 11(7):585–93. doi:10.1038/ni.1889

22. Crozat K, Guiton R, Contreras V, Feuillet V, Dutertre CA, Ventre E, et al. The XC chemokine receptor 1 is a conserved selective marker of mammalian cells homologous to mouse CD8alpha+ dendritic cells. *J Exp Med* (2010) 207(6):1283–92. doi:10.1084/jem.20100223

23. Haniffa M, Collin M, Ginhoux F. Ontogeny and functional specialization of dendritic cells in human and mouse. *Adv Immunol* (2013) 120:1–49. doi:10.1016/B978-0-12-417028-5.00001-6

24. Collin M, Bigley V, Haniffa M, Hambleton S. Human dendritic cell deficiency: the missing ID? *Nat Rev Immunol* (2011) 11:575–83. doi:10.1038/nri3046

25. Vinh DC, Patel SY, Uzel G, Anderson VL, Freeman AF, Olivier KN, et al. Autosomal dominant and sporadic monocytopenia with susceptibility to mycobacteria, fungi, papillomaviruses, and myelodysplasia. *Blood* (2010) 115(8):1519–29. doi:10.1182/blood-2009-03-208629

26. Bigley V, Haniffa M, Doulatov S, Wang XN, Dickinson R, McGovern N, et al. The human syndrome of dendritic cell, monocyte, B and NK lymphoid deficiency. *J Exp Med* (2011) 208(2):227–34. doi:10.1084/jem.20101459

27. MacDonald KP, Munster DJ, Clark GJ, Dzionek A, Schmitz J, Hart DN. Characterization of human blood dendritic cell subsets. *Blood* (2002) 100(13):4512–20. doi:10.1182/blood-2001-11-0097

28. Segura E, Valladeau-Guilemond J, Donnadieu MH, Sastre-Garau X, Soumelis V, Amigorena S. Characterization of resident and migratory dendritic cells in human lymph nodes. *J Exp Med* (2012) 209(4):653–60. doi:10.1084/jem.20111457

29. Heidkamp GF, Sander J, Lehmann CHK, Heger L, Eissing N, Baranska A, et al. Human lymphoid organ dendritic cell identity is predominantly dictated by ontogeny, not tissue microenvironment. *Sci Immunol* (2016) 1(6):1–17. doi:10.1126/sciimmunol.aai7677

30. van Leeuwen-Kerkhoff N, Lundberg K, Westers TM, Kordasti S, Bontkes HJ, de Gruijl TD, et al. Transcriptional profiling reveals functional dichotomy between human slan + non-classical monocytes and myeloid dendritic cells. *J Leukoc Biol* (2017) 102(4):1055–68. doi:10.1189/jlb.3MA0117-037R

31. Ruben JM, van den Ancker W, Bontkes HJ, Westers TM, Hooijberg E, Ossenkoppele GJ, et al. Apoptotic blebs from leukemic cells as a preferred source of tumor-associated antigen for dendritic cell-based vaccines. *Cancer Immunol Immunother* (2014) 63(4):335–45. doi:10.1007/s00262-013-1515-6

32. Hofer TP, Zawada AM, Frankenberger M, Skokann K, Satzl AA, Gesierich W, et al. Slan-defined subsets of CD16-positive monocytes: impact of granulomatous inflammation and M-CSF receptor mutation. *Blood* (2015) 126(24):2601–11. doi:10.1182/blood-2015-06-651331

33. Dzionek A, Fuchs A, Schmidt P, Cremer S, Zysk M, Miltenyi S, et al. BDCA-2, BDCA-3, and BDCA-4: three markers for distinct subsets of dendritic cells in human peripheral blood. *J Immunol* (2000) 165(11):6037–46. doi:10.4049/jimmunol.165.11.6037

34. Hémont C, Neel A, Heslan M, Braudeau C, Josien R. Human blood mDC subsets exhibit distinct TLR repertoire and responsiveness. *J Leukoc Biol* (2013) 93(4):599–609. doi:10.1189/jlb.0912452

35. Lindstedt M, Lundberg K, Borrebaeck CAK. Gene family clustering identifies functionally associated subsets of human in vivo blood and tonsillar dendritic cells. *J Immunol* (2005) 175(8):4839–46. doi:10.4049/jimmunol.175.8.4839

36. Lundberg K, Rydnert F, Greiff L, Lindstedt M. Human blood dendritic cell subsets exhibit discriminative pattern recognition receptor profiles. *Immunology* (2014) 142(2):279–88. doi:10.1111/imm.12252

37. Schäkel K, Kannagi R, Kniep B, Goto Y, Mitsuoka C, Zwirner J, et al. 6-Sulfo LacNAc, a novel carbohydrate modification of PSGL-1, defines an inflammatory type of human dendritic cells. *Immunity* (2002) 17(3):289–301. doi:10.1016/S1074-7613(02)00393-X

38. Schäkel K, von Kietzell M, Hänsel A, Ebling A, Schulze L, Haase M, et al. Human 6-sulfo LacNAc-expressing dendritic cells are principal producers of early interleukin-12 and are controlled by erythrocytes. *Immunity* (2006) 24(6):767–77. doi:10.1016/j.immuni.2006.03.020

39. Nizzoli G, Krietsch J, Weick A, Steinfelder S, Facciotti F, Gruarin P, et al. Human CD1c+ dendritic cells secrete high levels of IL-12 and potently prime cytotoxic T cell responses. *Blood* (2013) 122(6):932–42. doi:10.1182/blood-2013-04-495424

40. Breton G, Lee J, Liu K, Nussenzweig MC. Defining human dendritic cell progenitors by multiparametric flow cytometry. *Nat Protoc* (2015) 10(9):1407–22. doi:10.1038/nprot.2015.092

41. Kassianos AJ, Hardy MY, Ju X, Vijayan D, Ding Y, Vulink AJ, et al. Human CD1c (BDCA-1)+ myeloid dendritic cells secrete IL-10 and display an immuno-regulatory phenotype and function in response to *Escherichia coli*. *Eur J Immunol* (2012) 42(6):1512–22. doi:10.1002/eji.201142098

42. Patterson S, Donaghy H, Amjadi P, Gazzard B, Gotch F, Kelleher P. Human BDCA-1 positive blood dendritic cells differentiate into phenotypically distinct immature and mature populations in the absence of exogenous maturational stimuli: differentiation failure in HIV infection. *J Immunol* (2005) 174(12):8200–9. doi:10.4049/jimmunol.174.12.8200

43. Piccioli D, Tavarini S, Borgogni E, Steri V, Nuti S, Sammicheli C, et al. Functional specialization of human circulating CD16 and CD1c myeloid dendritic-cell subsets. *Blood* (2007) 109(12):5371–9. doi:10.1182/blood-2006-08-038422

44. Poulin LF, Reyal Y, Uronen-Hansson H, Schraml BU, Sancho D, Murphy KM, et al. DNGR-1 is a specific and universal marker of mouse and human Batf3-dependent dendritic cells in lymphoid and nonlymphoid tissues. *Blood* (2012) 119(25):6052–62. doi:10.1182/blood-2012-01-406967

45. Schäkel K, Mayer E, Federle C, Schmitz M, Riethmüller G, Rieber EP. A novel dendritic cell population in human blood: one-step immunomagnetic isolation by a specific mAb (M-DC8) and in vitro priming of cytotoxic T lymphocytes. *Eur J Immunol* (1998) 28(12):4084–93. doi:10.1002/(SICI)1521-4141(199812)28:12<4084::AID-IMMU4084>3.0.CO;2-4

46. Karsunky H, Merad M, Cozzio A, Weissman IL, Manz MG. Flt3 ligand regulates dendritic cell development from Flt3+ lymphoid and myeloid-committed progenitors to Flt3+ dendritic cells in vivo. *J Exp Med* (2003) 198(2):305–13. doi:10.1084/jem.20030323

47. McKenna HJ, Stocking KL, Miller RE, Brasel K, De Smedt T, Maraskovsky E, et al. Mice lacking flt3 ligand have deficient hematopoiesis affecting

hematopoietic progenitor cells, dendritic cells, and natural killer cells. *Blood* (2000) 95(11):3489–97.

48. Waskow C, Liu K, Darrasse-Jèze G, Guermonprez P, Ginhoux F, Merad M, et al. The receptor tyrosine kinase Flt3 is required for dendritic cell development in peripheral lymphoid tissues. *Nat Immunol* (2008) 9(6):676–83. doi:10.1038/ni.1615

49. Dong R, Cwynarski K, Entwistle A, Marelli-Berg F, Dazzi F, Simpson E, et al. Dendritic cells from CML patients have altered actin organization, reduced antigen processing, and impaired migration. *Blood* (2003) 101(9):3560–7. doi:10.1182/blood-2002-06-1841

50. Ma L, Delforge M, van Duppen V, Verhoef G, Emanuel B, Boogaerts M, et al. Circulating myeloid and lymphoid precursor dendritic cells are clonally involved in myelodysplastic syndromes. *Leukemia* (2004) 18(9):1451–6. doi:10.1038/sj.leu.2403430

51. Ma L, Ceuppens J, Kasran A, Delforge M, Boogaerts M, Vandenberghe P. Immature and mature monocyte-derived dendritic cells in myelodysplastic syndromes of subtypes refractory anemia or refractory anemia with ringed sideroblasts display an altered cytokine profile. *Leuk Res* (2007) 31(10): 1373–82. doi:10.1016/j.leukres.2006.11.007

52. Matteo Rigolin G, Howard J, Buggins A, Sneddon C, Castoldi G, Hirst WJ, et al. Phenotypic and functional characteristics of monocyte-derived dendritic cells from patients with myelodysplastic syndromes. *Br J Haematol* (1999) 107(4):844–50. doi:10.1046/j.1365-2141.1999.01781.x

53. Micheva I, Thanopoulou E, Michalopoulou S, Karakantza M, Kouraklis-Symeonidis A, Mouzaki A, et al. Defective tumor necrosis factor alpha-induced maturation of monocyte-derived dendritic cells in patients with myelodysplastic syndromes. *Clin Immunol* (2004) 113(3):310–7. doi:10.1016/j.clim.2004.08.007

54. Mohty M, Jarrossay D, Lafage-Pochitaloff M, Zandotti C, Brière F, de Lamballeri XN, et al. Circulating blood dendritic cells from myeloid leukemia patients display quantitative and cytogenetic abnormalities as well as functional impairment. *Blood* (2001) 98(13):3750–6. doi:10.1182/blood.V98.13.3750

55. Dhodapkar KM, Barbuto S, Matthews P, Kukreja A, Mazumder A, Vesole D, et al. Dendritic cells mediate the induction of polyfunctional human IL17-producing cells (Th17-1 cells) enriched in the bone marrow of patients with myeloma. *Blood* (2008) 112(7):2878–85. doi:10.1182/blood-2008-03-143222

56. Saft L, Björklund E, Berg E, Hellström-Lindberg E, Porwit A. Bone marrow dendritic cells are reduced in patients with high-risk myelodysplastic syndromes. *Leuk Res* (2013) 37(3):266–73. doi:10.1016/j.leukres.2012.10.010

57. Leone P, Berardi S, Frassanito MA, Ria R, De Re V, Cicco S, et al. Dendritic cells accumulate in the bone marrow of myeloma patients where they protect tumor plasma cells from CD8+ T-cell killing. *Blood* (2015) 126(12):1443–51. doi:10.1182/blood-2015-01-623975